# Electronic supplementary information

# AlbiCDN: Albumin-binding Amphiphilic STING Agonists Augments the Immune Activity for Cancer Immunotherapy

Shao-Hua Zhuo[a+], Xi Chen[b+], Lang Zhao[a], Tian-Yang Wang[a], Jing-Yun Su[a], Tao Yang[h,i,j,k], Lijun Yang[f,g], Fei Dong[l], Yu-Fen Zhao[a,e], and Yan-Mei Li[a,c,d*]

[a] Key Lab of Bioorganic Phosphorus Chemistry & Chemical Biology, Department of Chemistry, Tsinghua University, Beijing 100084, P. R. China. E-mail: liym@mail.tsinghua.edu.cn

[b] Zhili College, Tsinghua University, Beijing 100084, P. R. China

[c] Beijing Institute for Brain Disorders, Beijing 100069, P. R. China

[d] Center for Synthetic and Systems Biology, Tsinghua University, Beijing 100084, P. R. China

[e] Institute of Drug Discovery Technology, Ningbo University, Ningbo 315221, Zhejiang, P. R. China

[f] Higher Education Key Laboratory of Tumor Immunology & Targeted Drug Development in Shanxi Province, Shanxi Medical University, Taiyuan 030001, Shanxi, P. R. China

[g] Department of Pharmacology, Shanxi Medical University, Taiyuan 030001, Shanxi, P. R. China

[h] Key laboratory of Digestive Disease & Organ Transplantation in Shanxi Province, The First Hospital of Shanxi Medical University, Taiyuan 030001, Shanxi, P. R. China

[i] Higher Education Key Laboratory of Tumor Immunology & Targeted Drug Development in Shanxi Province, Shanxi Medical University, Taiyuan 030001, Shanxi, P. R. China

[j] Department of Biochemistry & Molecular Biology, Shanxi Medical University, Taiyuan 030001, Shanxi, P. R. China

[k] Key laboratory of Cellular Physiology, Shanxi Medical University, Ministry of Education, Taiyuan 030001, Shanxi, P. R. China

[l] Department of Hematology, Lymphoma Research Center, Peking University Third Hospital, Beijing 100191, P R China

[+] These authors contributed equally.

*Corresponding Author: liym@mail.tsinghua.edu.cn

# Table of Contents

## 1. Materials

Penicillin-streptomycin and 0.25 % trypsin-EDTA were purchased from Sigma-Aldrich. DMEM (Dulbecco's modified Eagle's medium) and RPMI-1640 (Roswell Park Memorial Institute 1640) were purchased from Corning. Red blood cell lysis buffer (cat. no. R1010) was purchased from Solarbio. BSA-biotin were purchased from Solarbio (cat. no. SHB063). Cell Counting Kit-8 (CCK-8) was purchased from DOJINDO (cat. no. CK04). Lipofectamine 3000 Transfection Reagent (cat. no. L3000015) was purchased from Invitrogen. Dithiothreitol (DTT) was purchased from Solarbio. Cy5-NHS was purchased from Meilunbio (cat. no. MB12193-2). Cy7-NHS was purchased from shanghai yuanye Bio-Technology (cat. no. S85505).

## 2. Chemistry

The solvents and chemicals for chemical synthesis were used as purchased with no further purification. All of the solvents and chemicals for chemical synthesis were purchased from Bidepharm, Innochem, Nanjing Huijutong Biotechnology or Sigma-Aldrich. 1C8-1C14 were purified by Silica gel column chromatography. CDG-1C8-CDG-1C14 were purified by high performance liquid chromatography (HPLC), and characterized by Thermo Scientific UltiMate 3000 (ESI-MS). HPLC analysis was performed with a linear gradient (5 % B/A (0 min) to 90 % B/A (30 min), and then 100 % B (30-40 min); flow rate = 4.0 mL/min) on a reversed-phase HPLC system (Shimadzu, SPD-20A) equipped with an YMC-Pack C8 column (OC12S05-2510WT, S-5 μm, 250X10.0 mml.D.). A: 0.05M triethylamine acetate, B: acetonitrile. The analyses of CDG-1C8-CDG-1C14 were performed on Shimadzu LC-2010A HPLC (YMC analytic C8 column) at a flow rate of 0.8 mL/min. $^{1}H$ and $^{13}C$ NMR spectra were collected by a JNM-ECZ400S/L1 400 MHz NMR spectrometer or a Bruker AV-HD-800X 800 MHz NMR spectrometer. $^{31}P$ spectra were collected by a JNM-ECA600 MHz NMR spectrometer and a JNM-ECZ400S/L1 400 MHz NMR spectrometer.

## 3. Supplementary Figure S1-S13

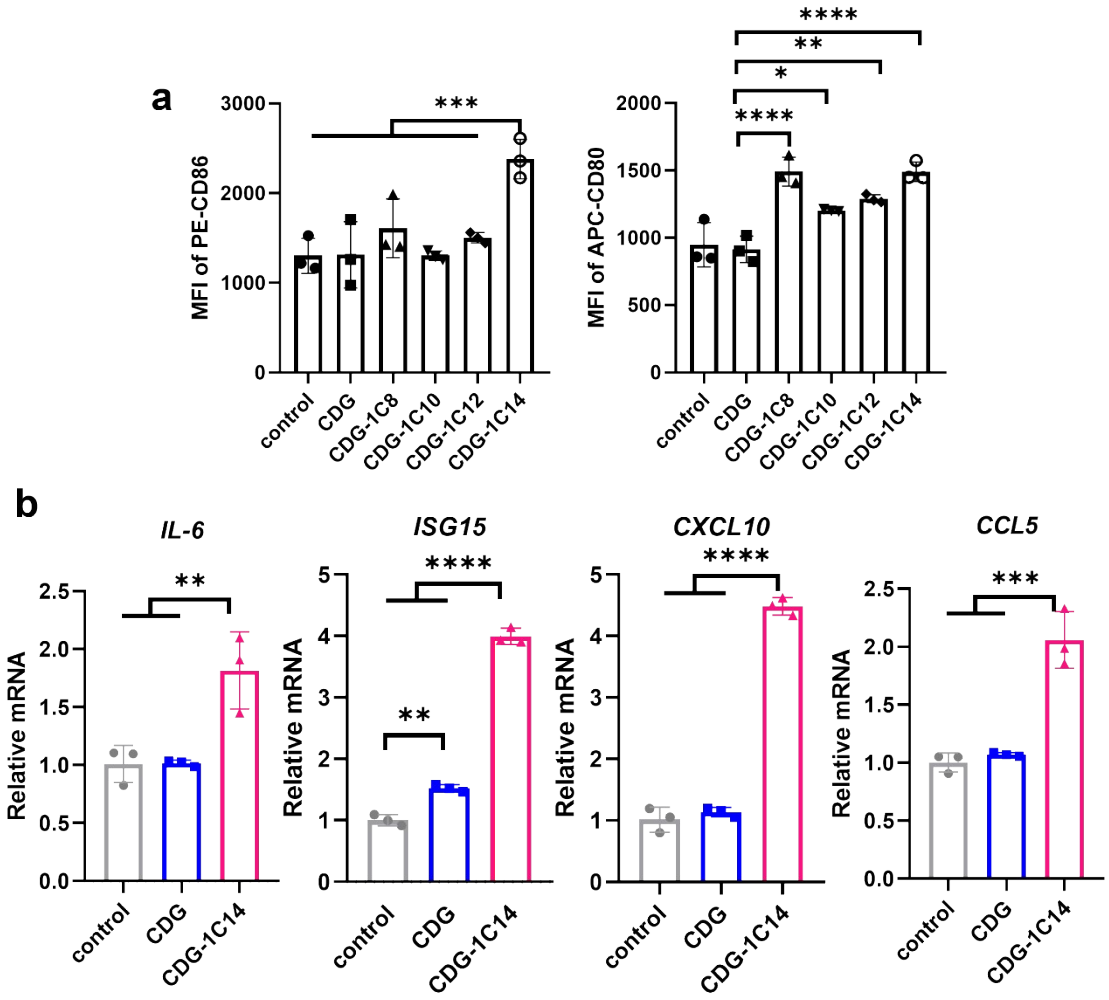


**Fig. S1.** CDG-1C14 significantly enhanced the immunostimulatory activity of CDG on MEF cells. **a**. The expression of CD86 and CD80 on MEF cells (n=3) with the treatment of AlbiCDN (5 μM). **b**. The expression of target genes *IL-6*, *ISG15*, CXCL10 and *CCL5* with the incubation of CDG-1C14 in MEF cells (n=3). Data are presented as mean ± SD. **P* < 0.05, ***P* < 0.01, ****P* < 0.001 and *****P* < 0.0001 were calculated by one-way ANOVA with Dunnett's multiple comparisons test. MFI, median fluorescence intensity.

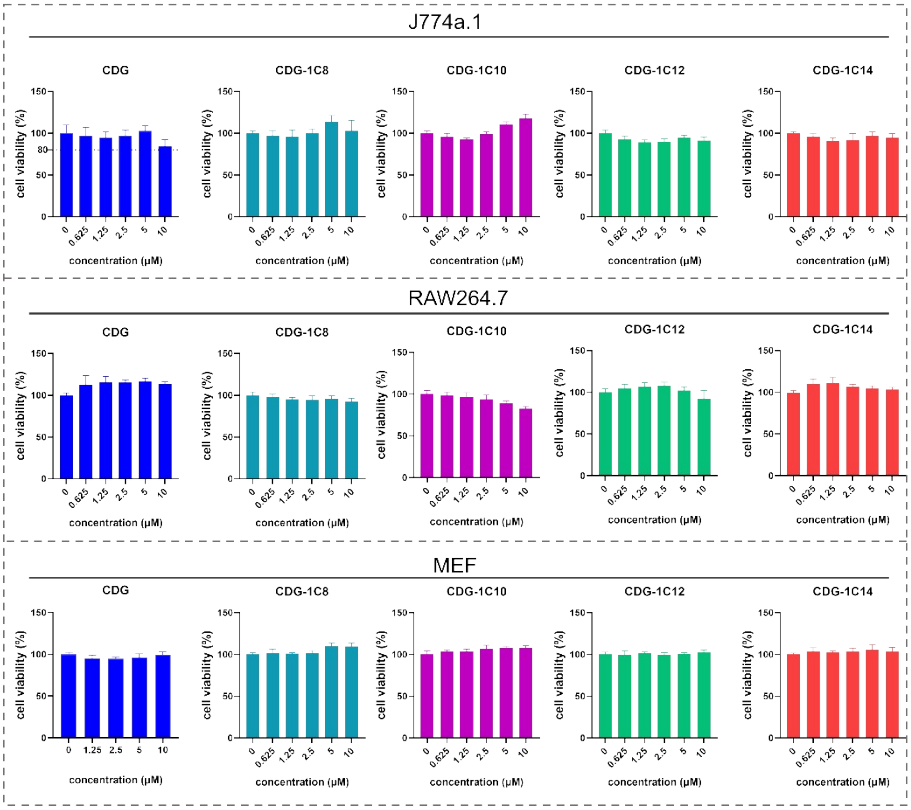


**Fig. S2.** The cell viability of AlbiCDN on J774A.1, RAW264.7 and MEF cells (n=5). Data are presented as mean ± SD.

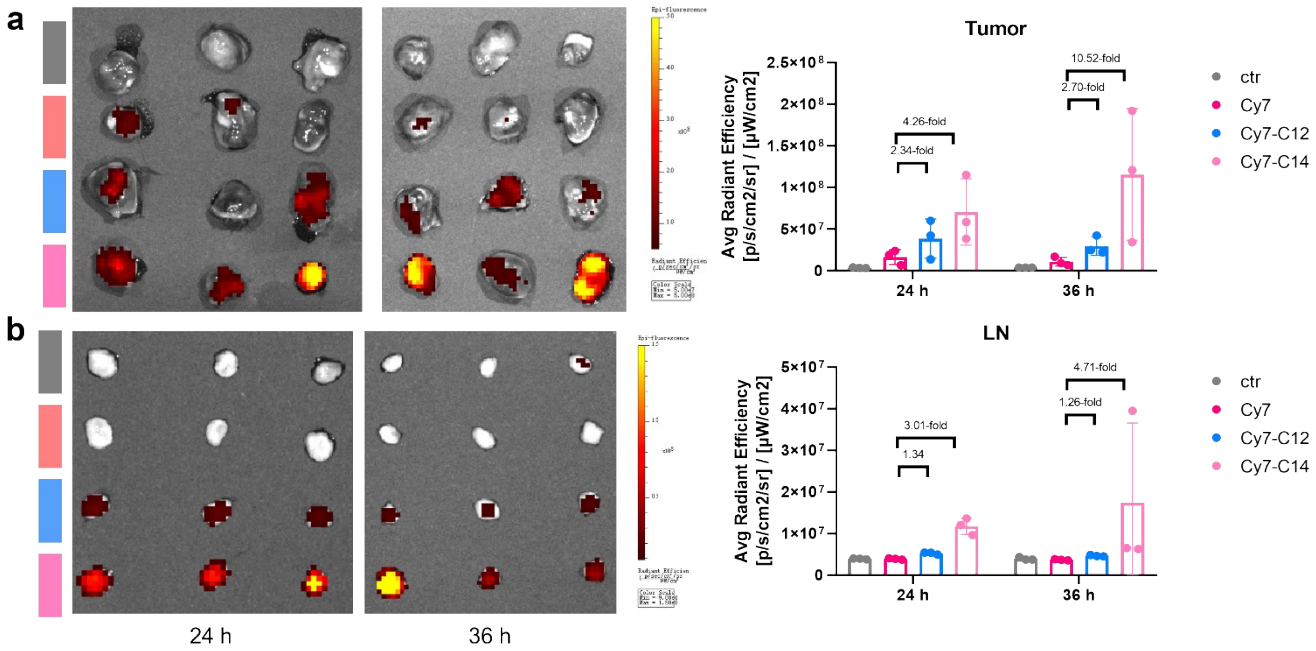


**Fig. S3.** IVIS fluorescence image and intensity quantification of tumour (**a**) and LNs (**b**) through i.v. (n=3). Data presented as mean ± SD.

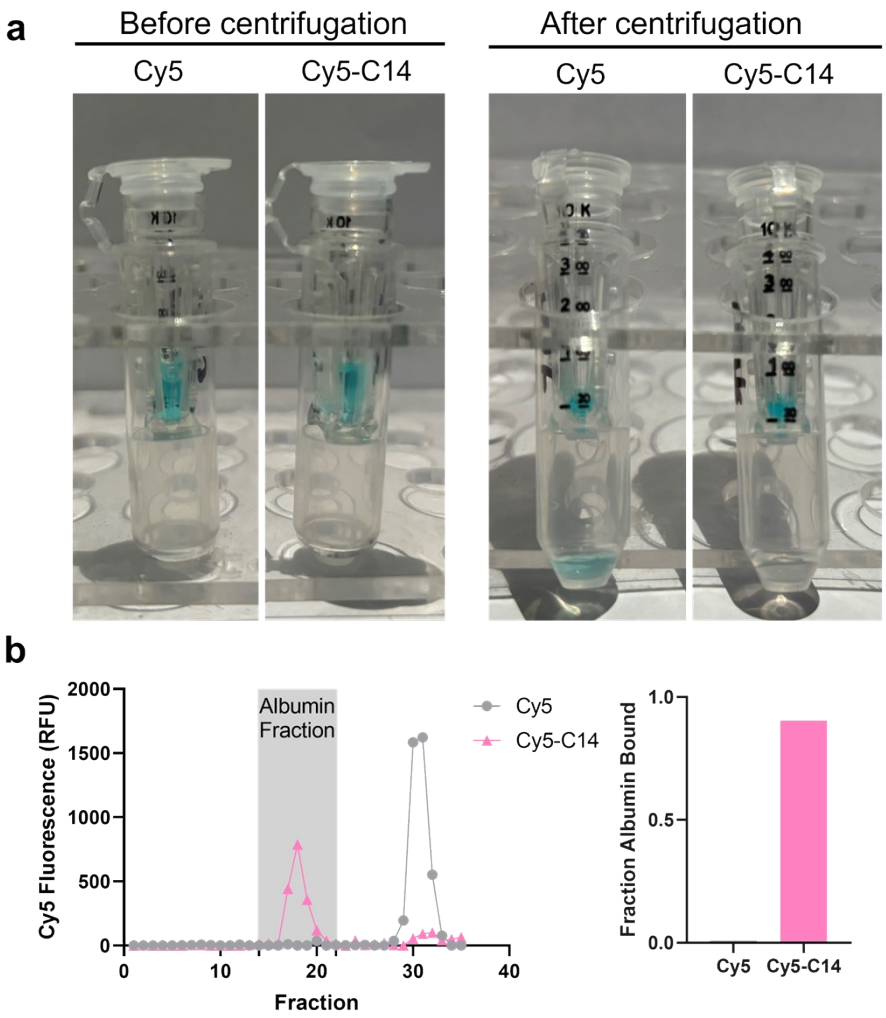


**Fig. S4**. **a.** Cy5 and Cy5-C14 were incubated with albumin for 1 h at 37 °C and the mixed solution was separated by filtration. Left: before centrifugation; right: after centrifugation. **b.** Cy5 fluorescence within the albumin-containing fractions was quantitated relative to the total serum fluorescence by size exclusion chromatography.

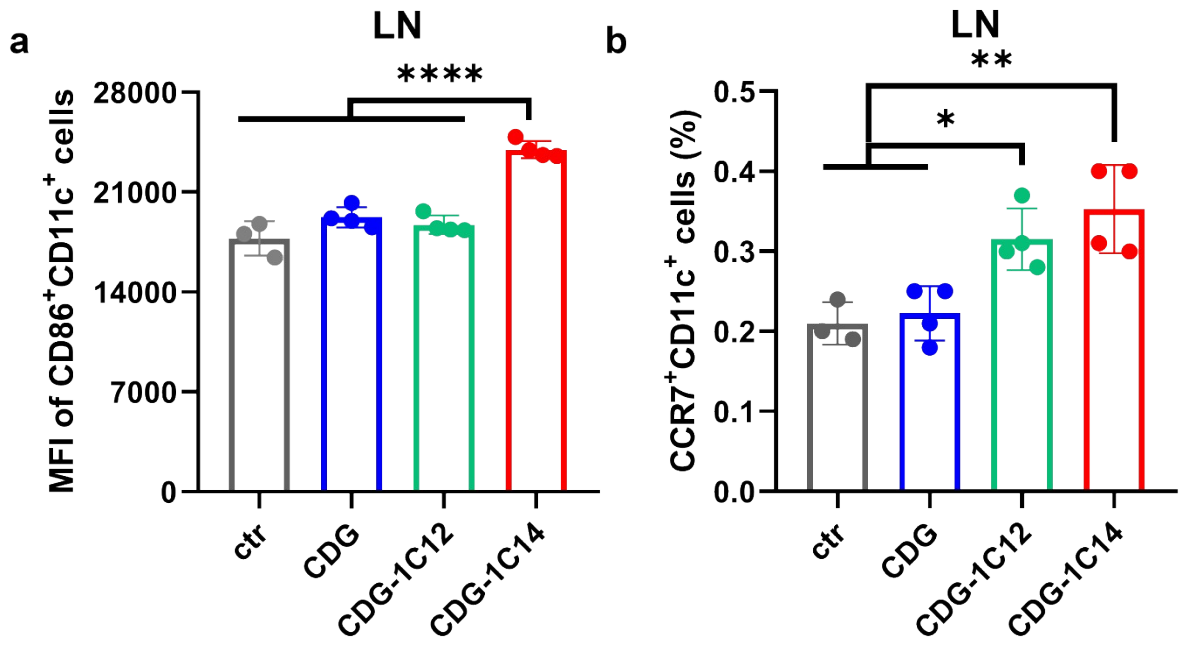


**Fig. S5. a.** Quantification of CD86 expression by DCs in LN. **b.** The evaluation of migratory APCs in LNs. Data are presented as mean ± SD. **P* < 0.05, ***P* < 0.01, and *****P* < 0.0001. were calculated by one-way ANOVA with Dunnett's multiple comparisons test. MFI, median fluorescence intensity.

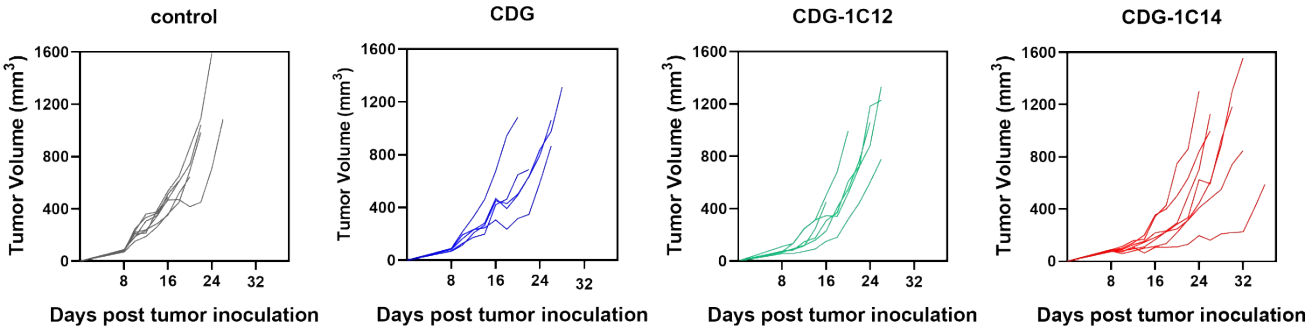


**Fig. S6.** Individual mice tumor volume through i.t. injection (related to Fig.5).

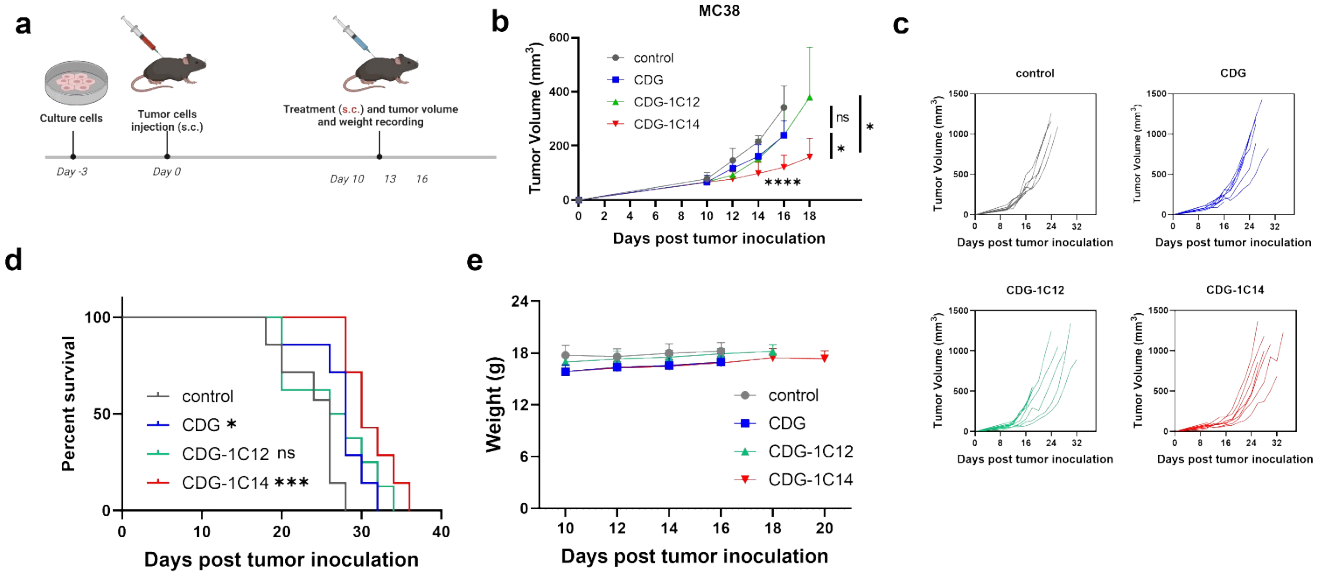


**Fig. S7. a**. Schematic of the therapeutic MC38 model through s.c. injection. Average tumor growth (**b**), individual mice tumour volume (**c**), survival curves (**d**), and mice weight (**f**) of MC38 tumor-bearing mice through i.t. injection. Data are presented as mean ± SD. Statistically significant differences for survival curves (c) were calculated using the Log-rank (Mantel-Cox) test. Other data were calculated using one-way ANOVA with Dunnett's multiple comparisons test. *$P < 0.05$ and ***$P < 0.001$. (**a**) were created with BioRender.

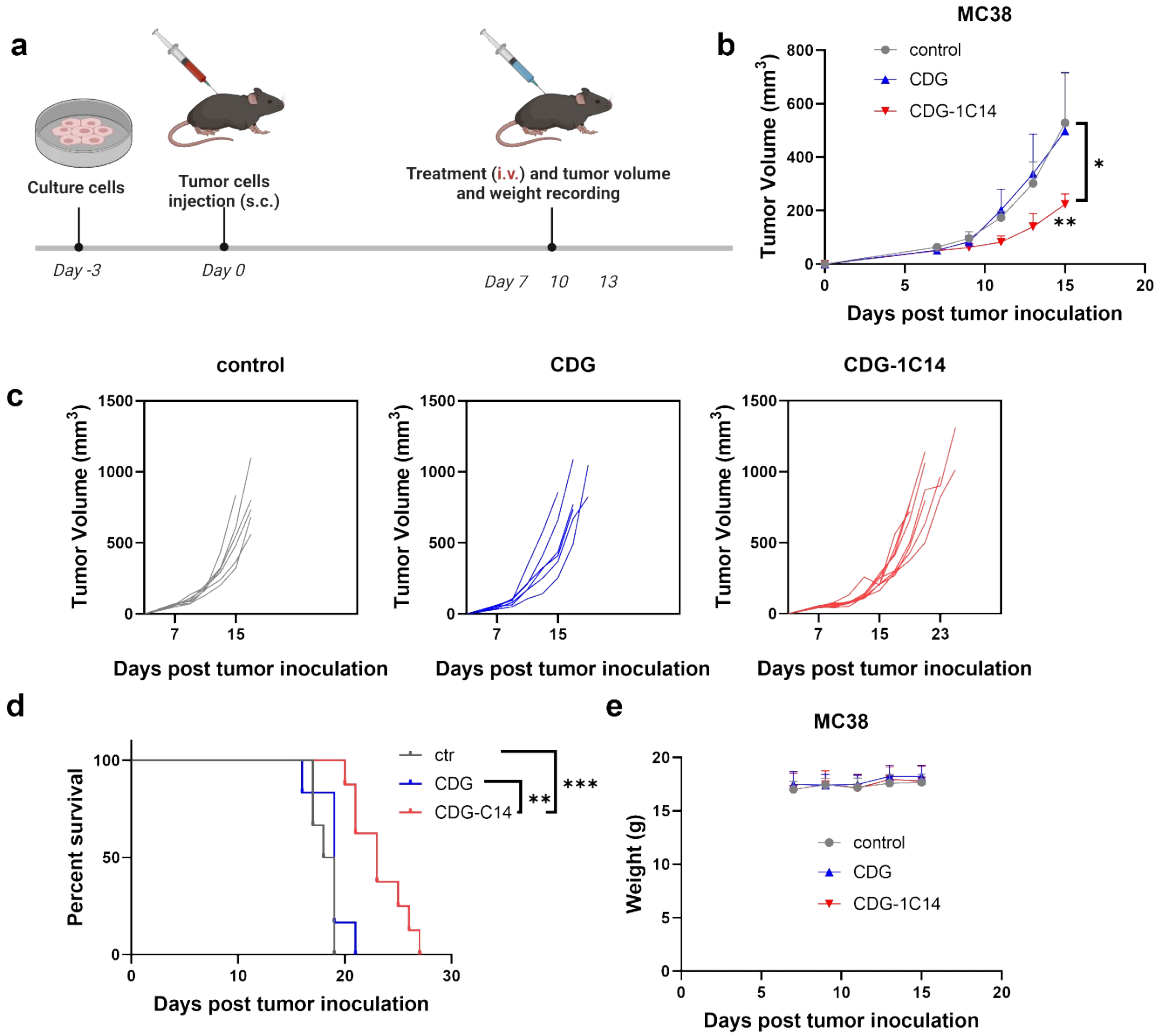


**Fig. S8. a**. Schematic of the therapeutic MC38 model through i.v. injection. Average tumour growth (**b**), individual mice tumour volume (**c**), survival curves (**d**), and mice weight (**f**) of MC38 tumor-bearing mice through i.t. injection. Data are presented as mean ± SD. Statistically significant differences for survival curves (c) were calculated using the Log-rank (Mantel-Cox) test. Other data were calculated using one-way ANOVA with Dunnett's multiple comparisons test. *$P < 0.05$, **$P < 0.01$, and ***$P < 0.001$. (**a**) were created with BioRender.

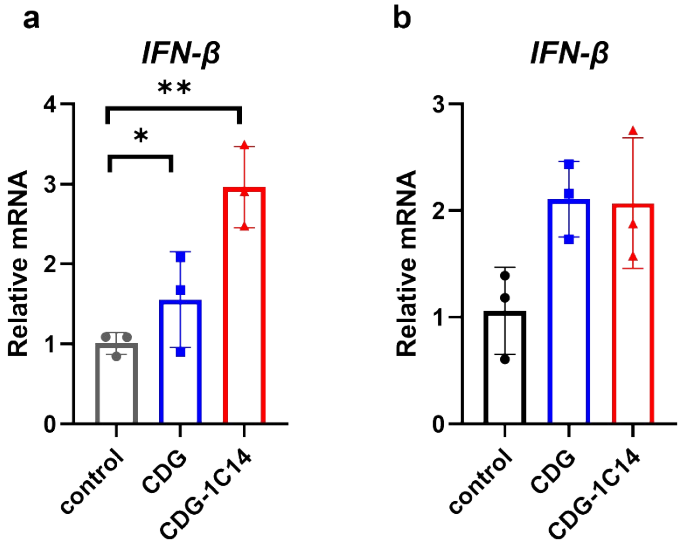

**Fig. S9. a-b**. Assessment of relative mRNA levels of target genes *IFN-β* (n = 3) in tumour (**a**) and LNs (**b**). Data were presented as mean ± SD. n, biologically independent experiments. $^{**}P < 0.05$, and $^{**}P < 0.01$. ns, no significant difference.

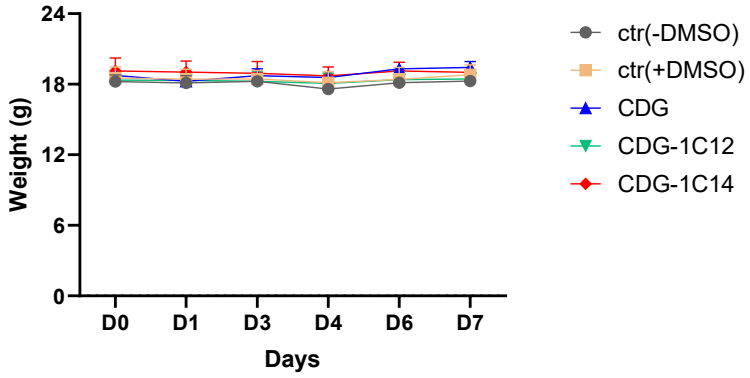


**Fig. S10.** The evaluation of biosafety of CDG-1C14 *in vivo* through the measurement of mice weight before and after s.c. injection (n=4)**.** The mice were randomly divided into five groups and injected (s.c.) with 100 μM CDG, 100 μM CDG-1C12, and 100 μM CDG-1C14 on days 0, 3, and 6. ctr (-DMSO) group: without DMSO; ctr (+DMSO) group: 1% DMSO (V/V). Data are presented as mean ± SD.

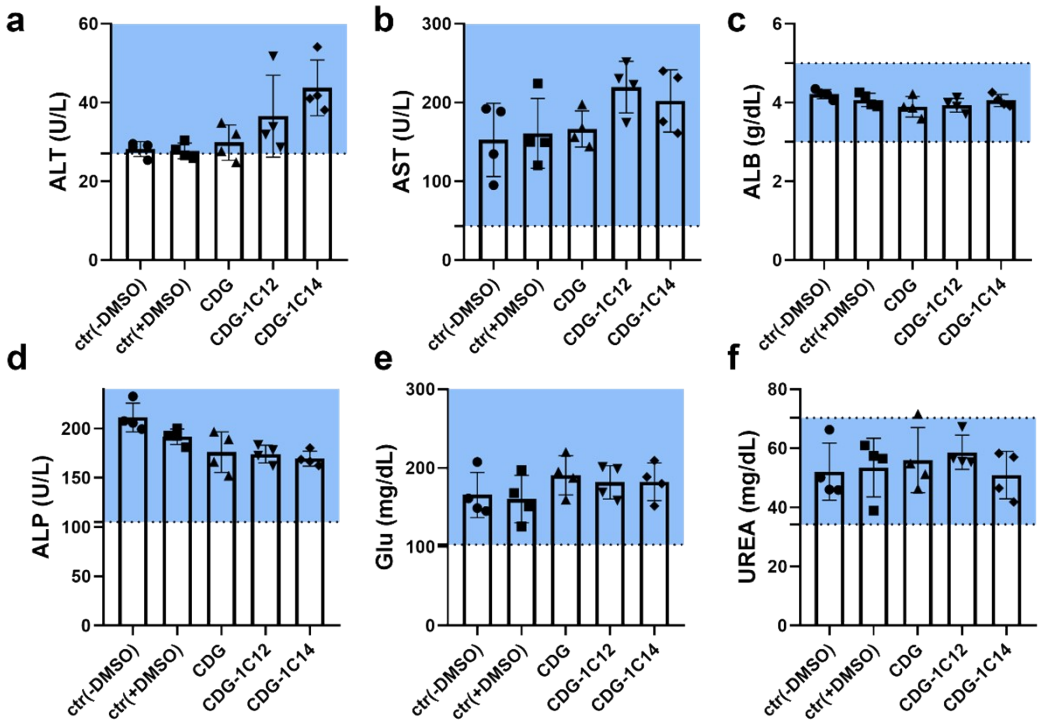


**Fig. S11.** The serum biochemistry evaluation of CDG-1C14 after the third immunization. **a**. Alanine aminotransferase (ALT). **b**. Aspartate aminotransferase (AST). **c**. Albumin (ALB). **d**. Alkaline phosphatase (ALP). **e**. Glucose (Glu). **f**. UREA. The blue shade related to the reported reference range of serum biochemistry on C57BL/6 mice. ctr (-DMSO) group: without DMSO; ctr (+DMSO) group: 1% DMSO (V/V); CDG group: 100 μM; CDG-1C12 group: 100 μM; CDG-1C14 group: 100 μM. Data are presented as mean ± SD.

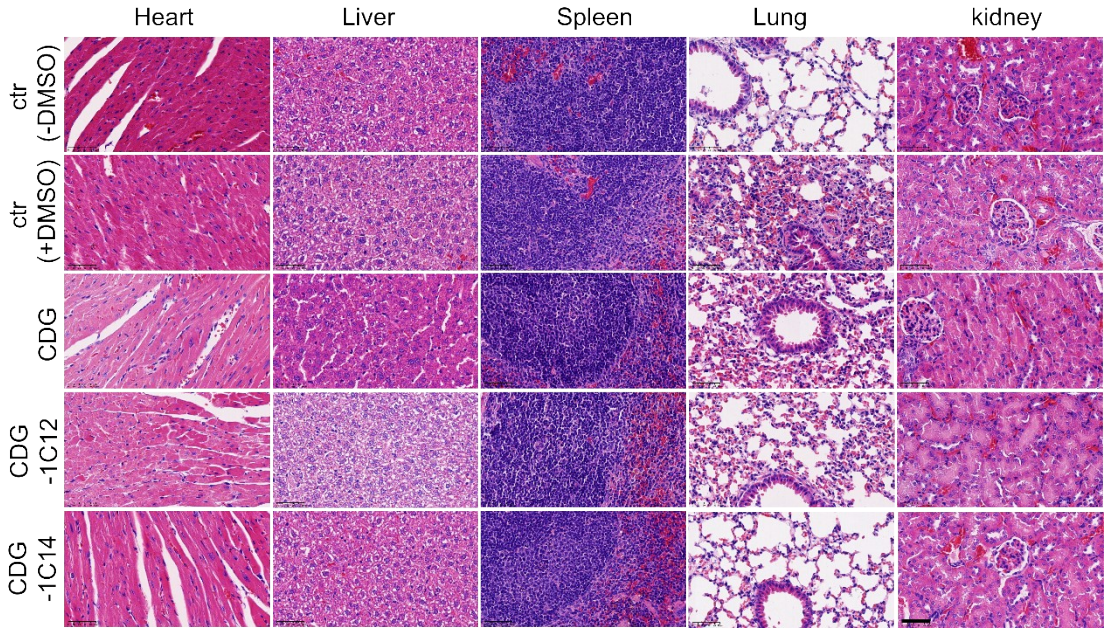


**Fig. S12.** The representative images of histological analysis after the third immunization.. Scar bars, 50 μm. ctr (-DMSO) group: without DMSO; ctr (+DMSO) group: 1% DMSO (V/V); CDG group: 100 μM; CDG-1C12 group: 100 μM; CDG-1C14 group: 100 μM.

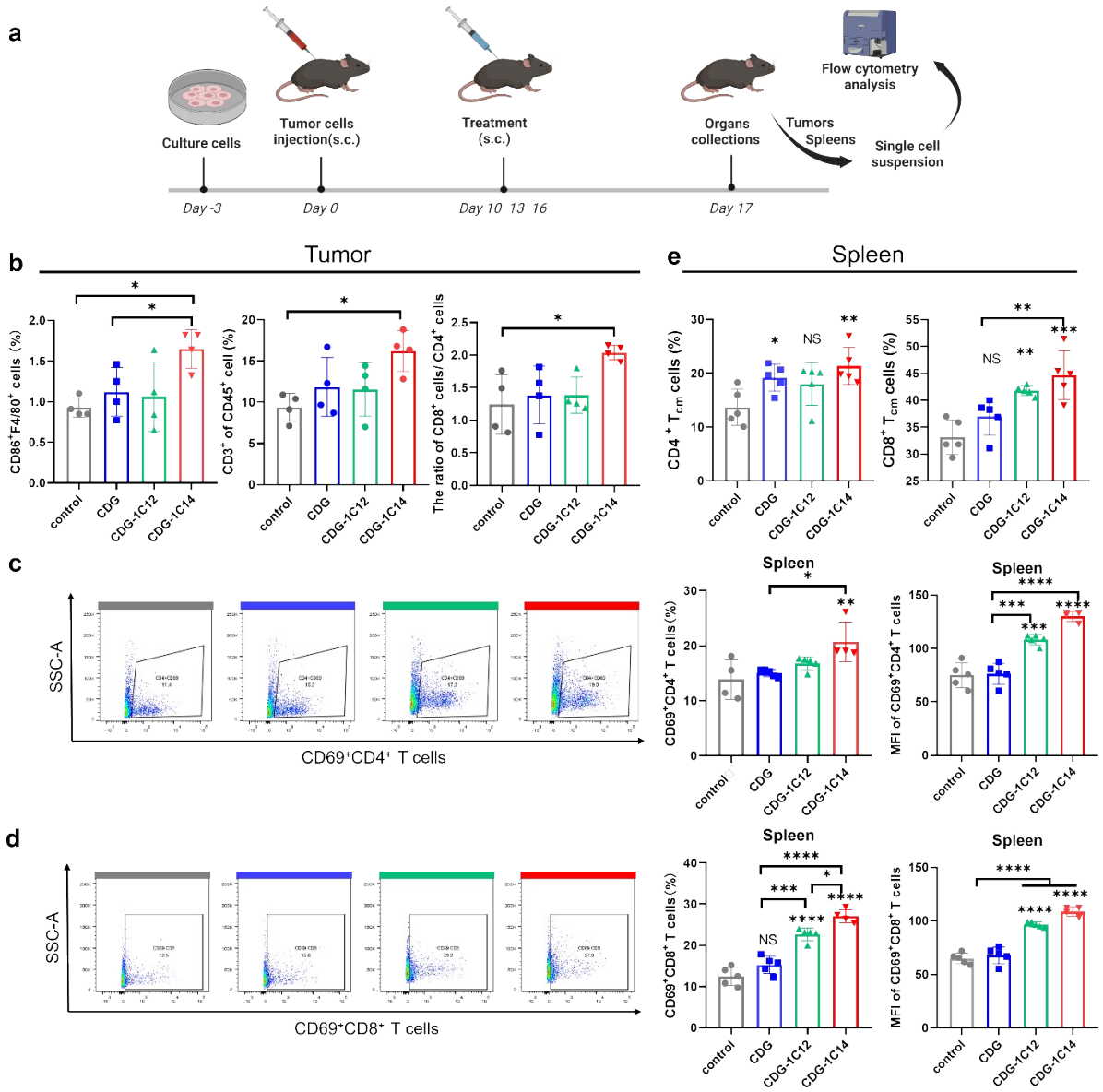


**Fig. S13.** CDG-1C14 induced an increase in tumor-infiltrating lymphocytes (TILs) and the generation of immune memory. **a**. Schematic of the MC38 tumor-bearing model for the analysis of immune response. **b**. Analysis of activated macrophages and infiltrating T cells in the TME (n=4). **c-d**. Analysis of activated T cells of splenic lymphocytes (n=4 or 5). Representative flow cytometry dot plot and quantification of CD69 expressions by splenic $CD4^+$ T cells (**c**) and $CD8^+$ T cells (**d**). **e**. Analysis of central memory T cells of splenic lymphocytes. (**a**) was created with BioRender. Data presented as mean ± SD. $*P < 0.05$, $**P < 0.01$, $***P < 0.001$, and $****P < 0.0001$ were calculated using one-way ANOVA with Dunnett's multiple comparisons test. ns, no significant difference. MFI, median fluorescence intensity.

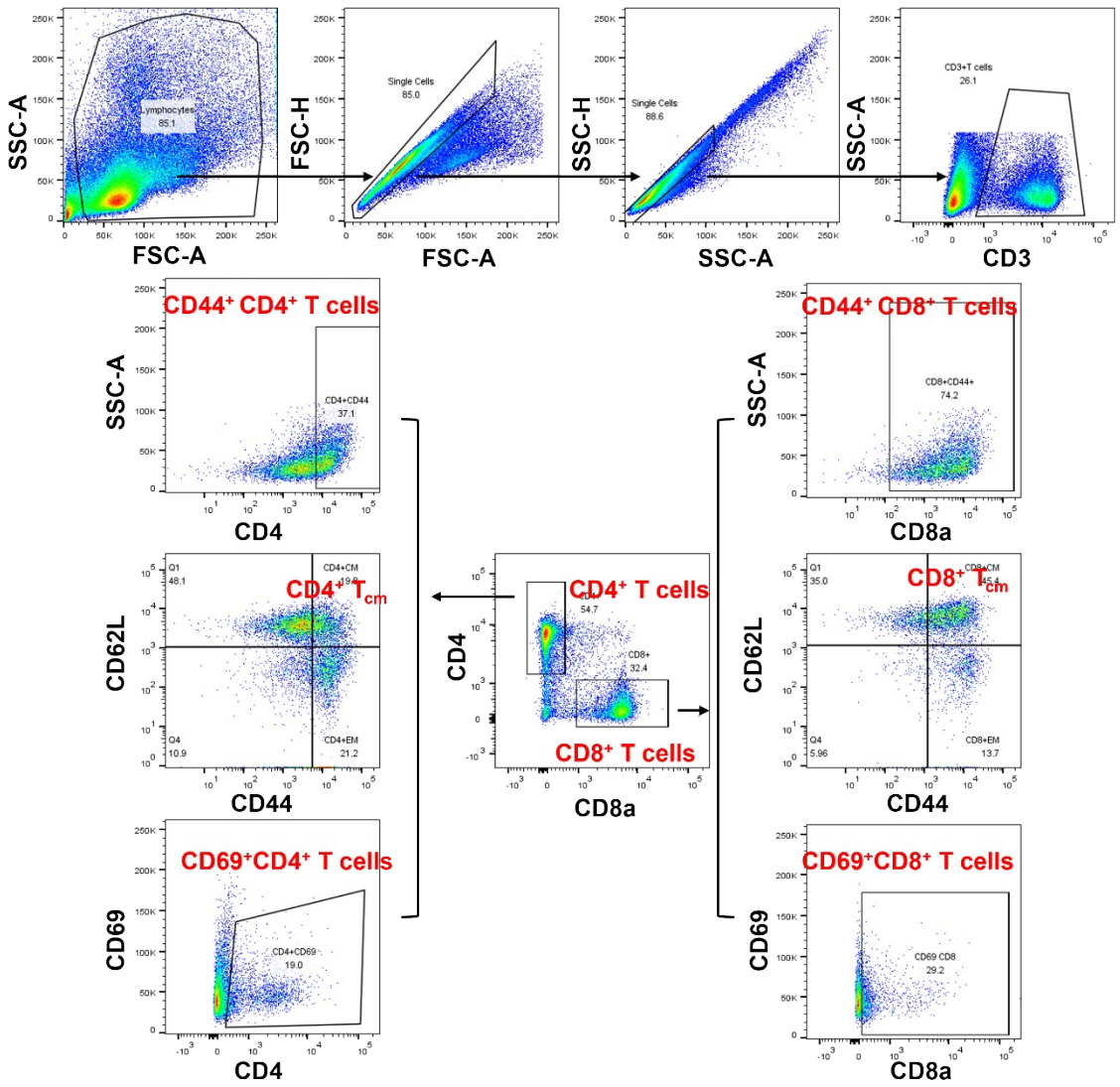


**Fig. S14.** Flow cytometry gating strategy for analysis of *in vivo* T cell activation and immune memory in spleens related to Fig. S13c-e.

## 4. Experimental method

**qPCR assay**

The extraction of total RNA from different cell line or tissures (Tumours or LNs) was carried out utilizing the Tissue Cell RNA Extraction Kit, which employs the Trizol method, Shanghai Yuanye Bio-Technology Co., Ltd, cat. No. R30506-50T). The assessment of RNA sample quality, as well as the processes of reverse transcription and quantitative real-time PCR, were conducted by Beijing Ruibio BioTech Co., Ltd. The SYBR Green primers used in this study were also custom synthesized by Beijing Ruibio BioTech. The relative expression levels of genes were determined using the ΔΔCt approach, with expression levels normalized to the Hprt gene.

The following primer sequences were used:

| | |
|---|---|
| Hprt Forward | TGAAGTACTCATTATAGTCAAGGGCA |
| Hprt Reverse | CTGGTGAAAAGGACCTCTCG |
| IFN-β Forward | GCCTTTGCCATCCAAGAGATGC |
| IFN-β Reverse | ACACTGTCTGCTGGTGGAGTTC |
| IL-6 Forward | GCCAGAGTCCTTCAGAGAGATACA |
| IL-6 Reverse | CTTGGTCCTTAGCCACTCCTTC |
| ISG15 Forward | CATCCTGGTGAGGAACGAAAGG |
| ISG15 Reverse | CTCAGCCAGAACTGGTCTTCGT |
| CXCL10 Forward | AGTGCTGCCGTCATTTTCTG |
| CXCL10 Reverse | ATTCTCACTGGCCCGTCA |
| CCL5 Forward | CCTGCTGCTTTGCCTACCTCTC |
| CCL5 Reverse | ACACACTTGGCGGTTCCTTCGA |
| STING Forward | GGTCACCGCTCCAAATATGTAG |
| STING Reverse | CAGTAGTCCAAGTTCGTGCGA |
| TBK1 Forward | GACATGCCTCTCTCCTGTAGTC |
| TBK1 Reverse | GGTGAAGCACATCACTGGTCTC |
| IRF3 Forward | CGGAAAGAAGTGTTGCGGTTAGC |
| IRF3 Reverse | CAGGCTGCTTTTGCCATTGGTG |
| NF-κB Forward | ATGGCAGACGATGATCCCTAC |
| NF-κB Reverse | CGGAATCGAAATCCCCTCTGTT |

## 5. Chemical protocols and NMR data

**Procedures for the synthesis of compound 1C8-1C14.**

To a solution of cystamine dihydrochloride (456 mg, 2.0 mmol, 1.0 equiv) and $K_2CO_3$ (884 mg, 6.4 mmol, 3.2 equiv) in acetonitrile (30 mL) was added slowly 1-bromooctane (347 mg, 1.8 mmol, 0.9 equiv) at 50 °C. The reaction mixture was stirred overnight. The reaction was extracted with ethylacetate (3*50 mL). The combined organic layer was dried with $MgSO_4$ and concentrated under reduced pressure without further purification to yield 1C8 as a white powder. 1C10-1C14 were synthesized similarly to 1C8.

**1C8**

**$^1$H NMR (400 MHz, Chloroform-*d*)** δ 2.98 (t, *J* = 6.2 Hz, 2H), 2.91 (t, *J* = 6.4 Hz, 2H), 2.80 (t, *J* = 6.4 Hz, 2H), 2.73 (t, *J* = 6.2 Hz, 2H), 2.58 (t, *J* = 7.3 Hz, 2H), 1.73 (s, 3H), 1.56 - 1.36 (m, 3H), 1.35 - 1.09 (m, 10H), 0.84 (t, *J* = 6.8 Hz, 3H).

**$^{13}$C NMR (100 MHz, Chloroform-*d*)** δ 49.62, 48.10, 42.54, 40.61, 38.69, 31.88, 30.03, 29.56, 29.31, 27.38, 22.71, 14.16.

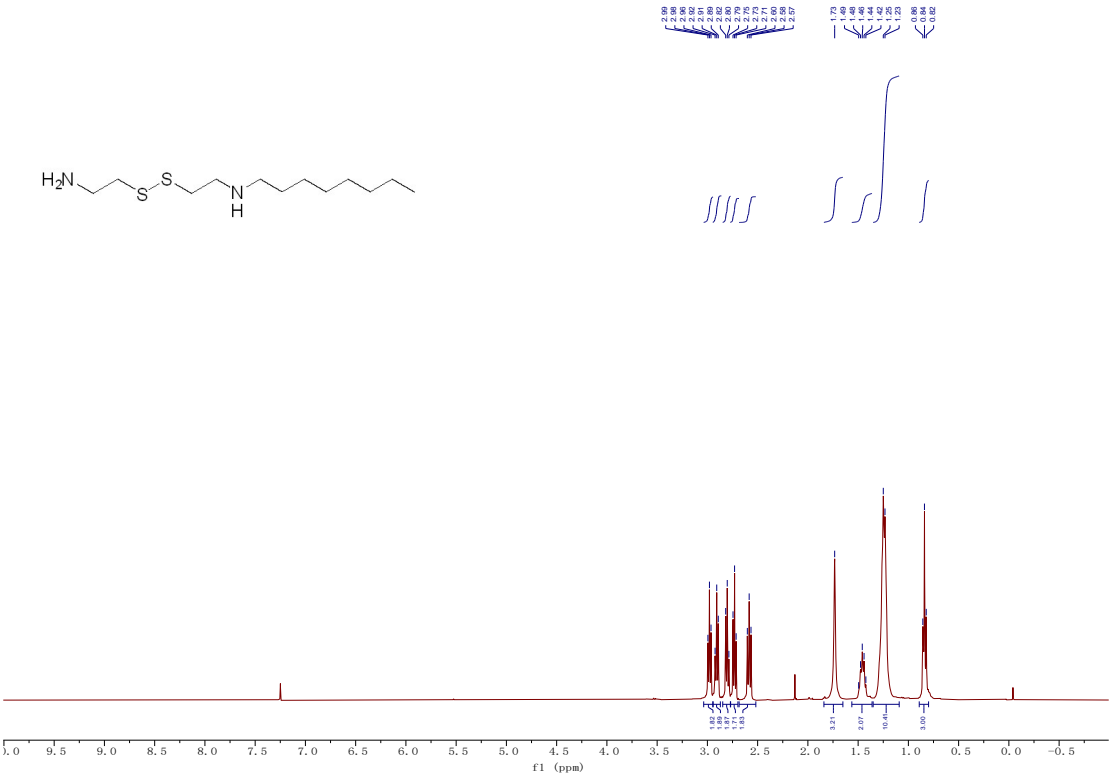


**Fig. S15.** $^1$H NMR (400 MHz, Chloroform-*d*) spectra of **1C8**.

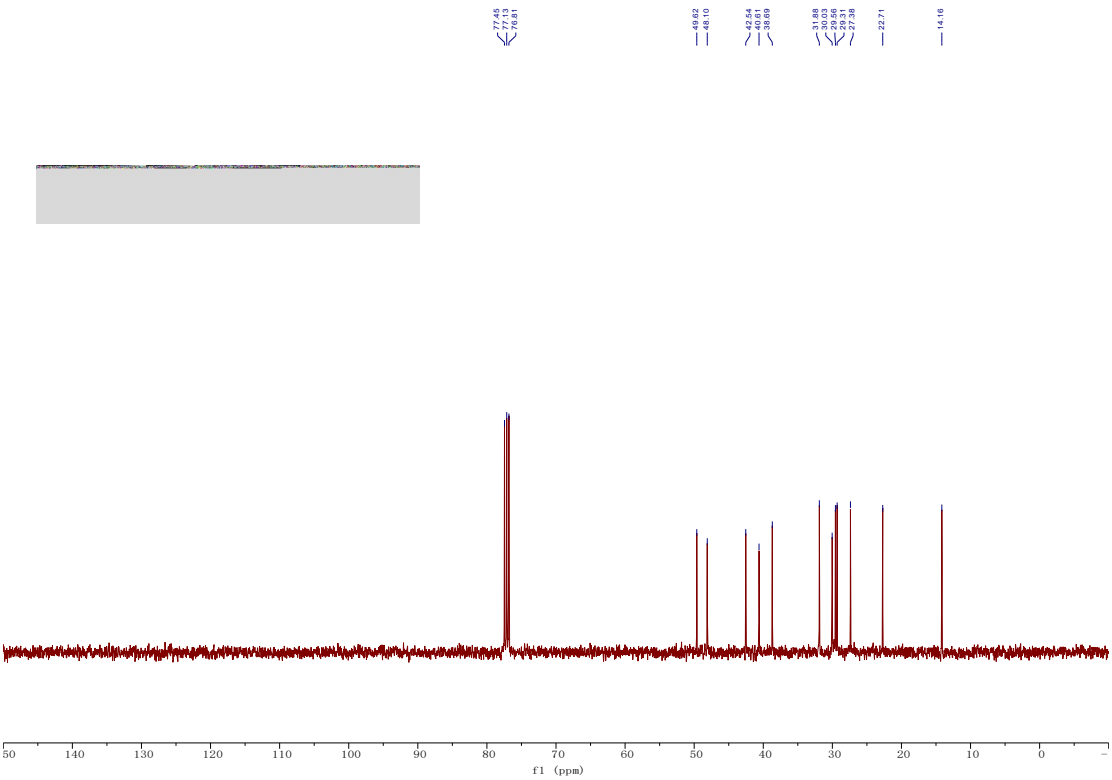

**Fig. S16.** $^{13}$C NMR (100 MHz, Chloroform-*d*) spectra of **1C8**.

**1C10**

**$^{1}$H NMR (400 MHz, Chloroform-*d*)** δ 2.99 (t, *J* = 6.2 Hz, 2H), 2.91 (t, *J* = 6.3 Hz, 2H), 2.81 (t, *J* = 6.4 Hz, 2H), 2.74 (t, *J* = 6.2 Hz, 2H), 2.68 – 2.49 (m, 2H), 1.53 (s, 3H), 1.50 - 1.40 (m, 2H), 1.30 - 1.17 (m, 14H), 0.85 (t, *J* = 6.8 Hz, 3H).

**$^{13}$C NMR (100 MHz, Chloroform-*d*)** δ 49.67, 48.14, 42.63, 40.65, 38.83, 31.97, 30.13, 29.67, 29.64, 29.63, 29.39, 27.41, 22.75, 14.18.

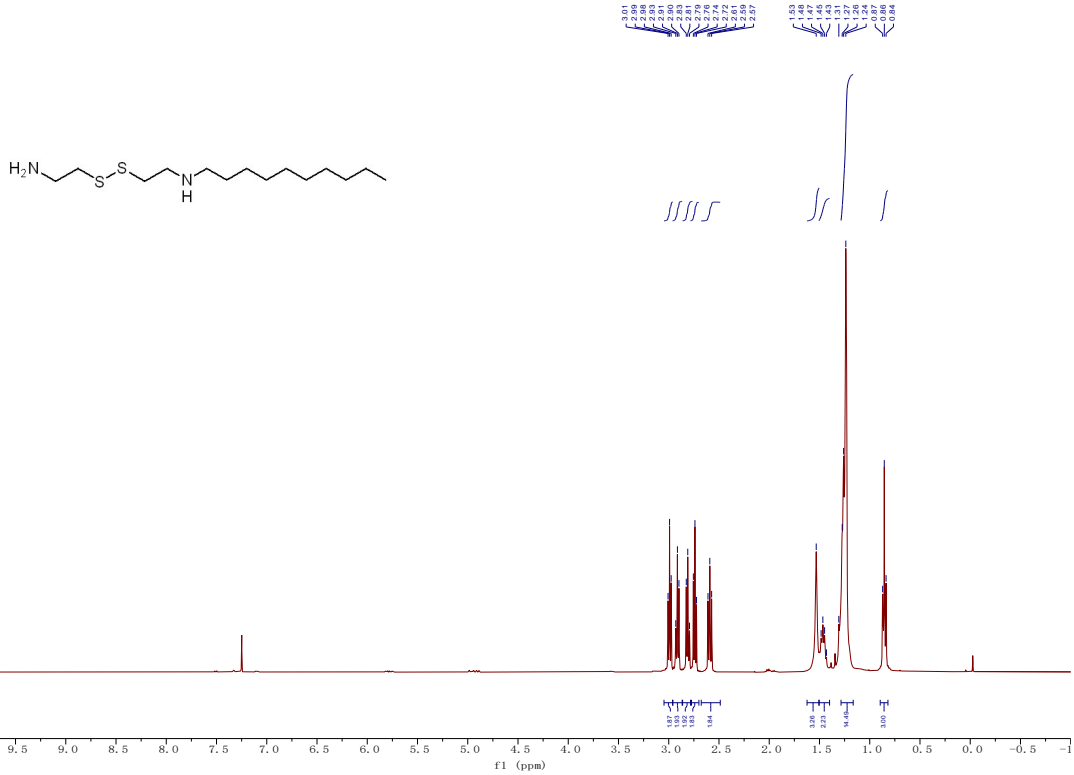

**Fig. S17.** [1]H NMR (400 MHz, Chloroform-*d*) spectra of **1C10**.

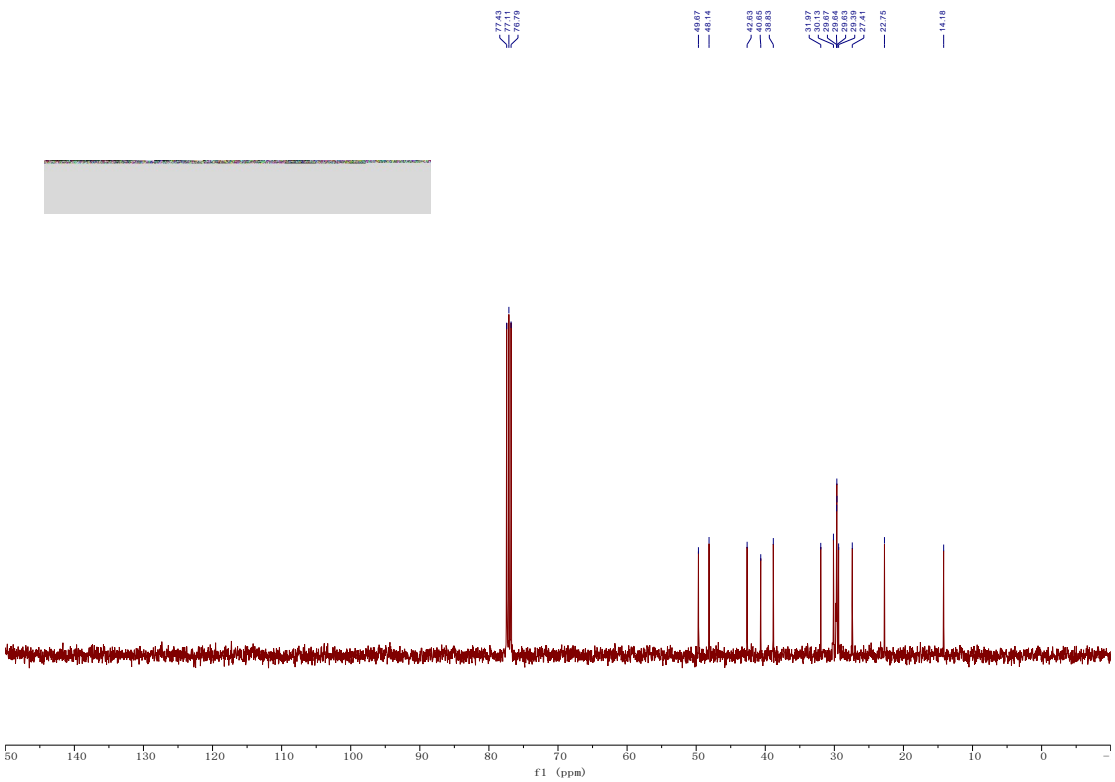


**Fig. S18.** [13]C NMR (100 MHz, Chloroform-*d*) spectra of **1C10**.

**1C12**

**[1]H NMR (400 MHz, Chloroform-*d*)** δ 2.99 (t, *J* = 6.2 Hz, 2H), 2.92 (t, *J* = 6.4 Hz, 2H), 2.81 (t, *J* = 6.2 Hz, 2H), 2.74 (t, *J* = 6.2 Hz, 2H), 2.66 - 2.55 (m, 2H), 1.53 (s, 3H), 1.50 - 1.41 (m, 2H), 1.20 - 1.21 (m, 18H), 0.86 (t, *J* = 6.8 Hz, 3H).

**[13]C NMR (100 MHz, Chloroform-*d*)** δ 49.69, 48.15, 42.65, 40.67, 38.87, 31.99, 30.16, 29.81, 29.73, 29.71, 29.69, 29.63, 29.42, 27.41, 22.76, 14.19.

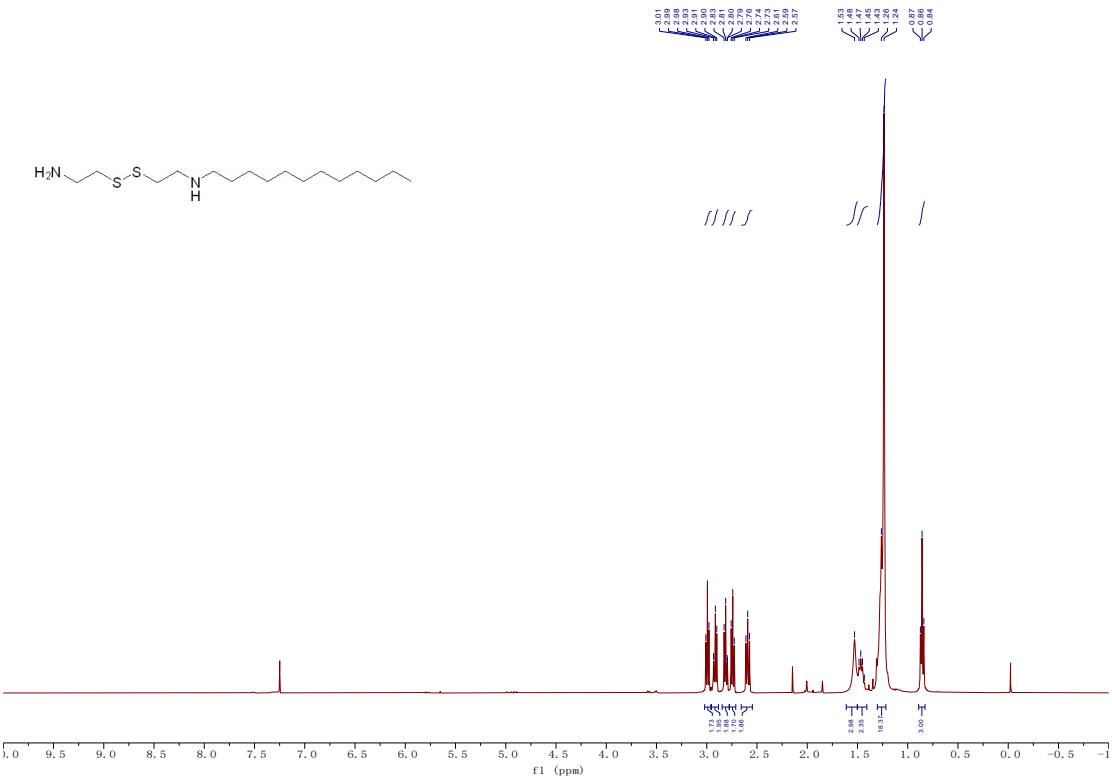

**Fig. S19.** $^{1}$H NMR (400 MHz, Chloroform-*d*) spectra of **1C12**.

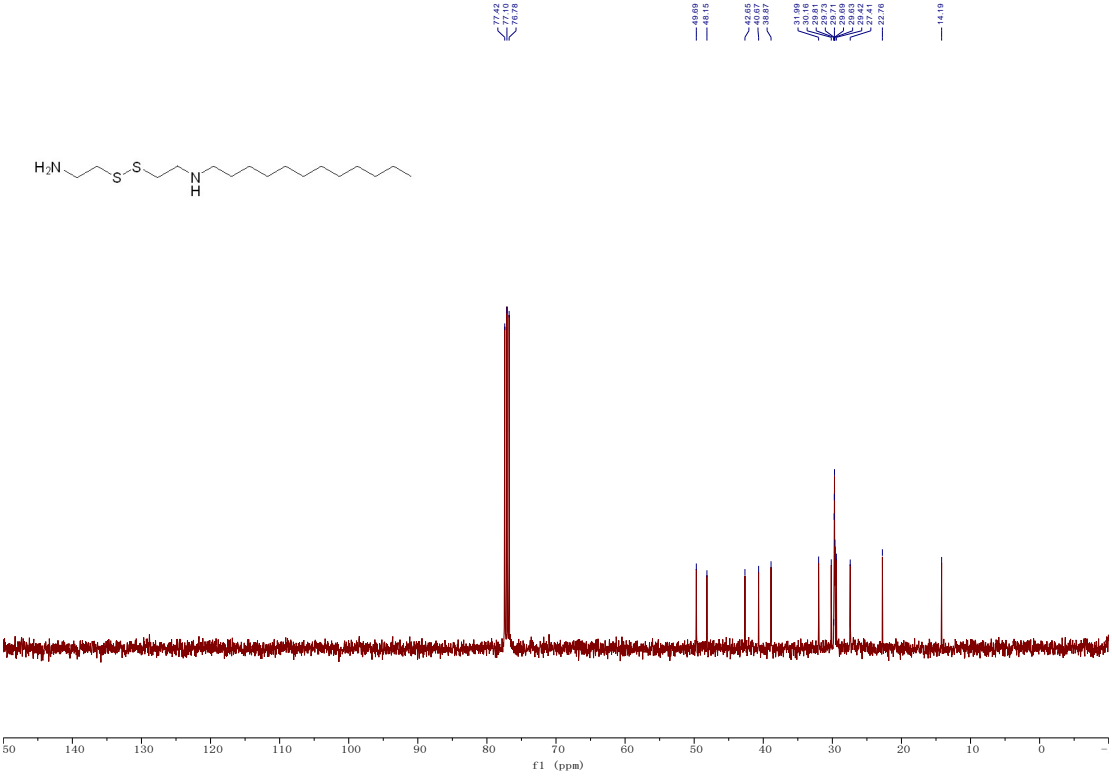

**Fig. S20.** $^{13}$C NMR (100 MHz, Chloroform-*d*) spectra of **1C12**.

**1C14**

**$^{1}$H NMR (400 MHz, Chloroform-*d*)** δ 2.99 (t, *J* = 6.2 Hz, 2H), 2.91 (t, *J* = 6.3 Hz, 2H), 2.81 (t, *J* = 6.3 Hz, 2H), 2.74 (t, *J* = 6.2 Hz, 2H), 2.59 (t, *J* = 7.2 Hz, 2H), 1.50 (s, 3H), 1.48 - 1.42 (m, 2H), 1.30 - 1.20 (m, 22H), 0.85 (t, *J* = 6.8 Hz, 3H).

**$^{13}$C NMR (100 MHz, Chloroform-*d*)** δ 49.69, 48.15, 42.65, 40.67, 38.90, 31.99, 30.18, 29.77, 29.76, 29.75, 29.73, 29.72, 29.69, 29.63, 29.43, 27.41, 22.76, 14.19.

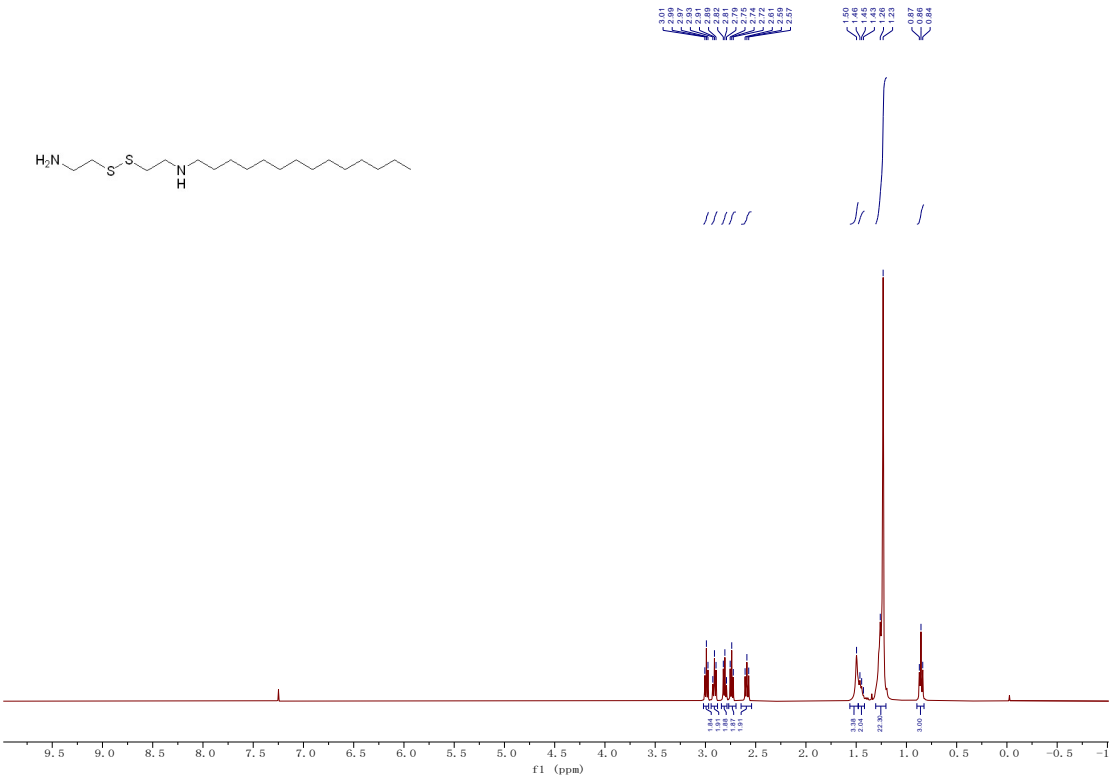


**Fig. S21.** $^{1}$H NMR (400 MHz, Chloroform-*d*) spectra of **1C14**.

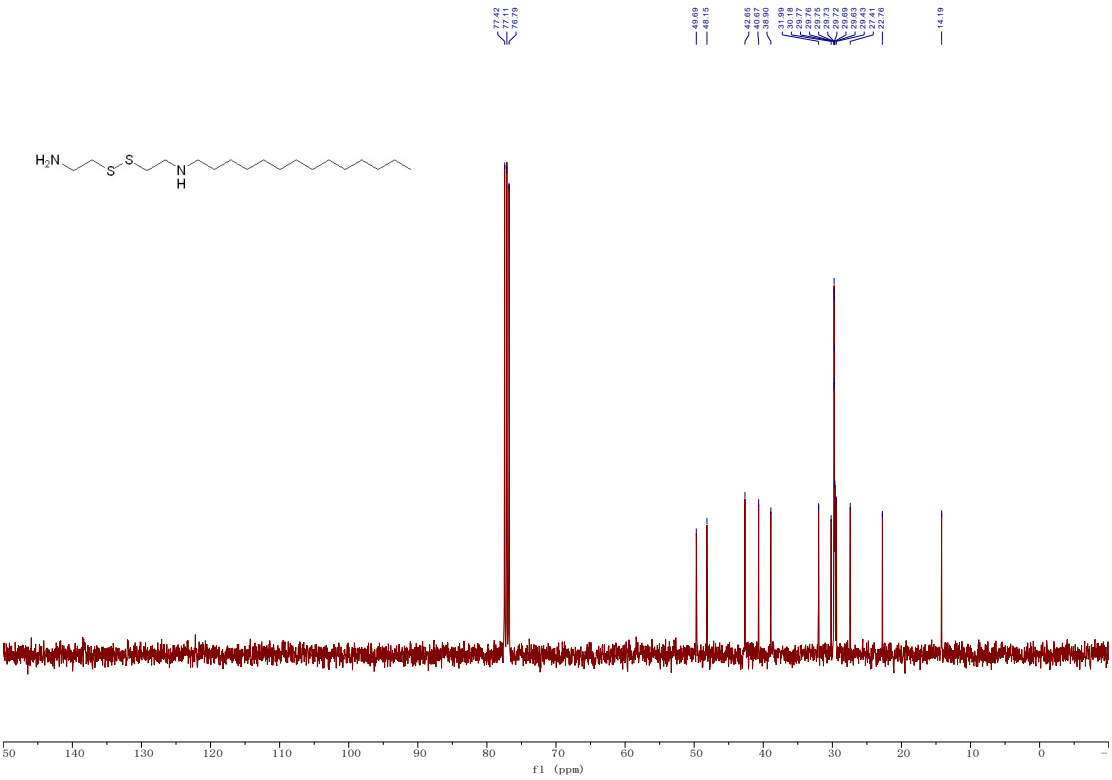

**Fig. S22.** $^{13}$C NMR (100 MHz, Chloroform-*d*) spectra of **1C14**.

## Procedures for the synthesis of compound CDG

CDG was synthesized according to the one-flask synthesis strategy as previously reported[1]. The detailed protocol has been described in their published papers. The crude product of CDG WASthen purified with HPLC (solution A: 0.05M triethylamine acetate, solution B: acetonitrile, pH=7.0, gradient is 5 % to 40 % of solution B in solution A in 30 min on the C18 column, 7.5 mL/min).

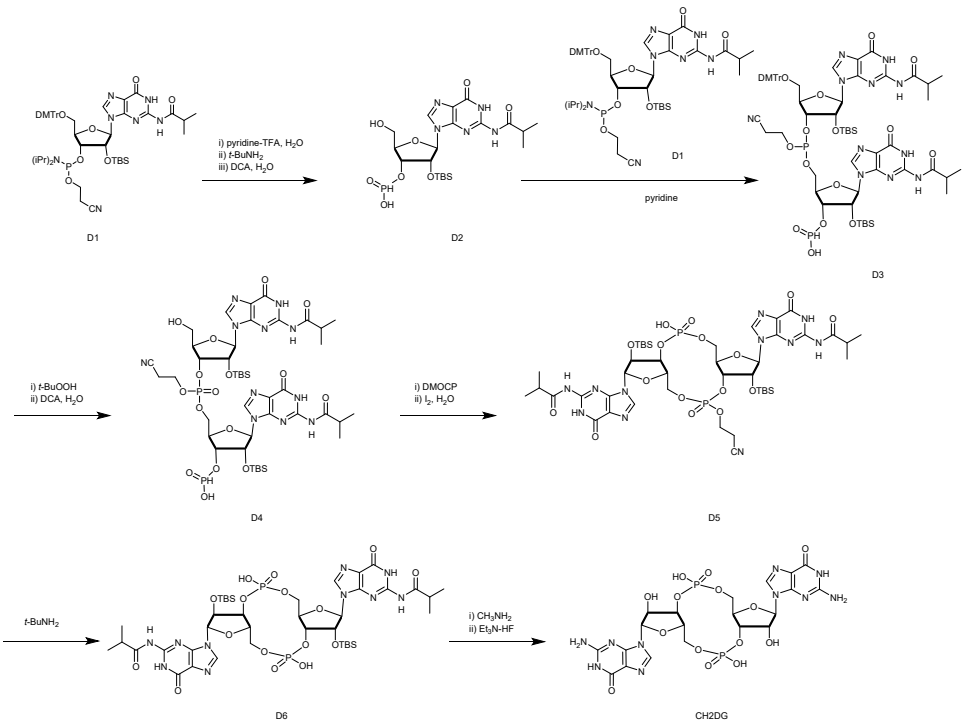


**Scheme S1.** Synthesis of CDG[1].

**CDG**

**$^{1}$H NMR (800 MHz, DMSO-$d_6$)** δ 7.97 (s, 2H), 6.64 (s, 2H), 5.73 (d, *J* = 6.7 Hz, 2H), 4.63 (d, *J* = 5.4 Hz, 4H), 4.14 (dd, *J* = 9.7, 4.2 Hz, 2H), 3.95 (p, *J* = 4.7 Hz, 2H). **$^{31}$P NMR (162 MHz, DMSO-$D_6$)** δ 0.43.

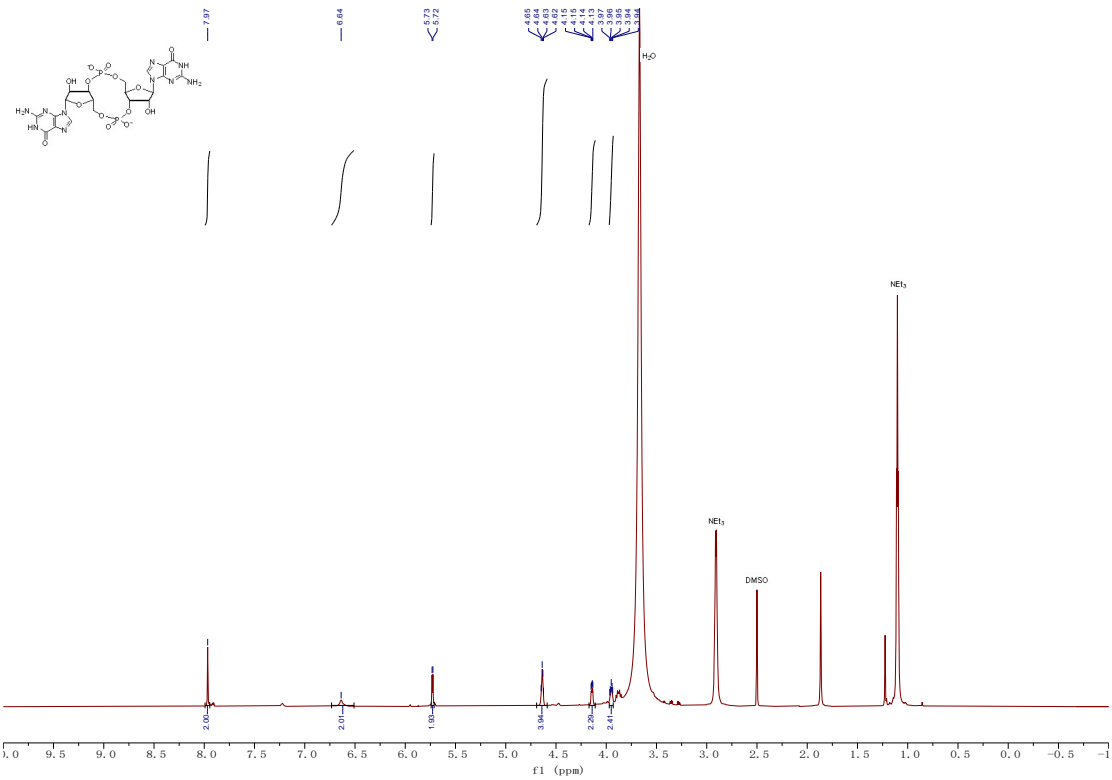


**Fig. S23.** $^{1}$H NMR (800 MHz, DMSO-$d_6$) spectra of **CDG**.

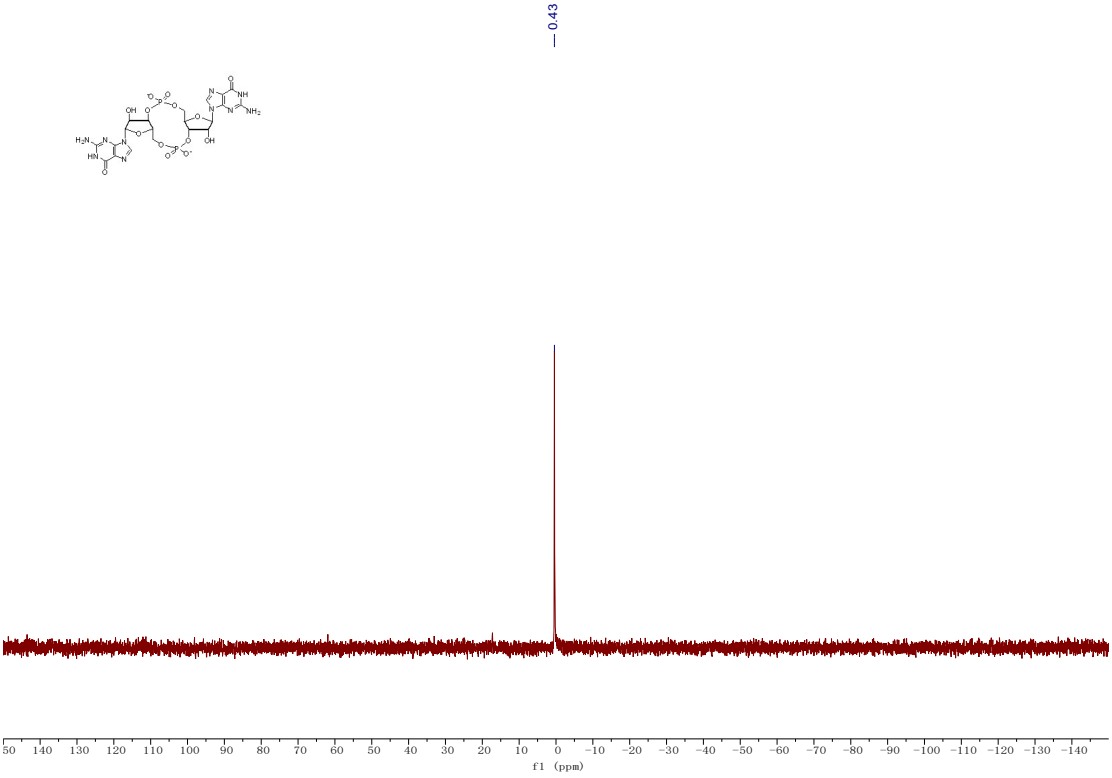


**Fig. S24.** $^{31}$P NMR (162 MHz, DMSO-$D_6$) spectra of **CDG**.

**Procedures for the synthesis of compound CDG-1Cn (n=8, 10, 12, 14).**

17.8 mg (0.02 mmol, 1.0 equiv) CDG was dissolved into 6 mL anhydrous N,N-Dimethylformamide (DMF). 6.4 mg (0.10 mmol, 5.0 equiv) CDI was dissolved in 100 μL anhydrous DMF. CDI solution was

added slowly to CDG solution forth times. The reaction was stirred at 37 ℃ for 12 h and monitored by ESI-MS. Without purification, 31.7 mg (0.12 mmol, 6.0 equiv) 1C8 were added to the solution and stirred overnight. The mixture was then purified with HPLC (solution A: 0.05M triethylamine acetate, solution B: acetonitrile, pH=7.0, gradient is 30 % to 90 % of solution B in solution A in 30 min on the C8 column, 4.0 mL/min) to obtain compound CDG-1C8. CDG-1C10-CDG-1C14 were synthesized similarly to CDG-1C8.

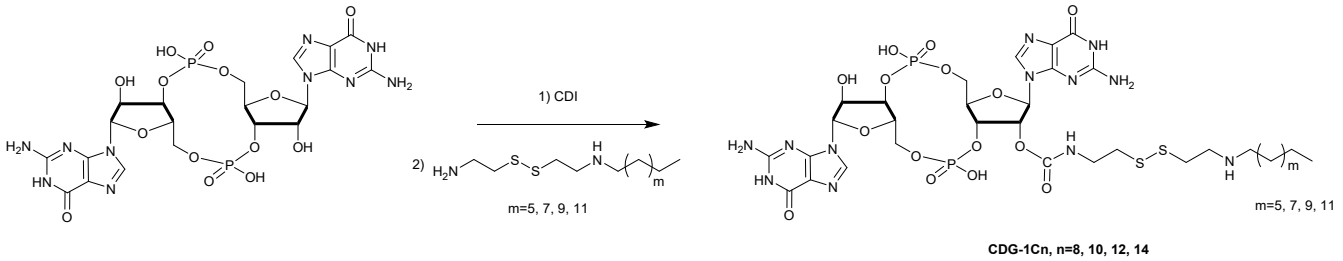


**Scheme S2**. Synthesis of **CDG-1Cn**.

**CDG-1C8**

**$^{1}$H NMR (800 MHz, DMSO-$d_6$)** δ 7.99 (s, 1H), 7.93 (s, 1H), 5.92 (d, *J* = 3.9 Hz, 1H), 5.72 (d, *J* = 6.4 Hz, 1H), 5.51 (d, *J* = 4.5 Hz, 1H), 5.33 (t, *J* = 5.0 Hz, 2H), 5.11 - 4.90 (m, 1H), 4.73 (p, *J* = 4.0 Hz, 1H), 4.47 (t, *J* = 5.9 Hz, 1H), 4.20 - 4.16 (m, 1H), 4.08 - 4.02 (m, 2H), 4.02 - 3.98 (m, 1H), 3.05 - 2.99 (m, 2H), 2.99 - 2.90 (m, 4H), 2.61 -2.52 (m, 4H), 1.52 - 1.44 (m, 2H), 1.35 - 1.25 (m, 10H), 0.86 (t, *J* = 7.0 Hz, 3H). **$^{31}$P NMR (162 MHz, DMSO-$D_6$)** δ -0.59, -1.25.

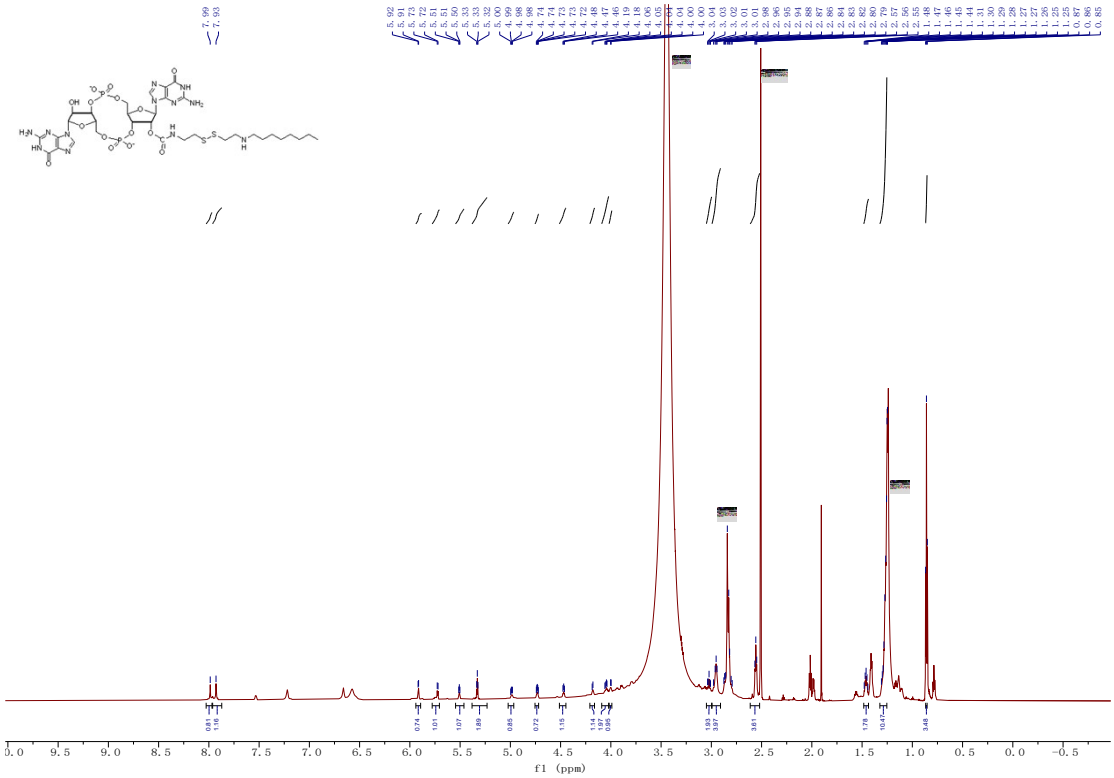


**Fig. S25.** $^{1}$H NMR (800 MHz, DMSO-$d_6$) spectra of **CDG-1C8**.

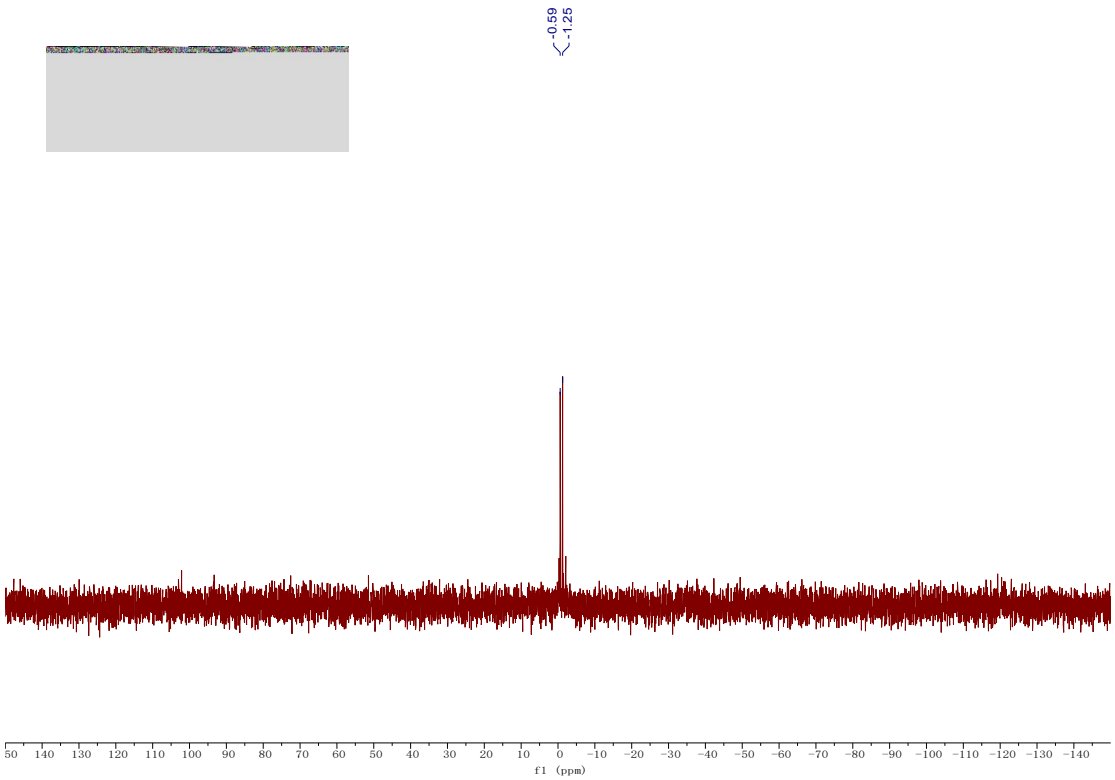


**Fig. S26.** $^{31}$P NMR (162 MHz, DMSO-$D_6$) spectra of **CDG-1C8**.

**CDG-1C10**

**$^{1}$H NMR (800 MHz, DMSO-$d_6$)** δ 7.96 (d, $J$ = 10.1 Hz, 2H), 5.87 (d, $J$ = 3.2 Hz, 1H), 5.73 (t, $J$ = 5.3 Hz, 1H), 5.55 - 5.48 (m, 1H), 5.31 (t, $J$ = 5.1 Hz, 2H), 4.96 (q, $J$ = 7.3, 6.9 Hz, 1H), 4.71 (q, $J$ = 5.6 Hz, 1H), 4.44 (t, $J$ = 4.9 Hz, 1H), 4.16 - 4.11 (m, 1H), 4.09 - 4.02 (m, 2H), 4.02 - 3.98 (m, 1H), 3.20 - 3.10 (m, 2H), 3.03 - 2.92 (m, 4H), 2.91 - 2.78 (m, 4H), 1.48 - 1.41 (m, 2H), 1.25 - 1.19 (m, 14H), 0.84 (t, $J$ = 7.0 Hz, 3H). **$^{31}$P NMR (162 MHz, DMSO-$D_6$)** δ -0.47, -1.11.

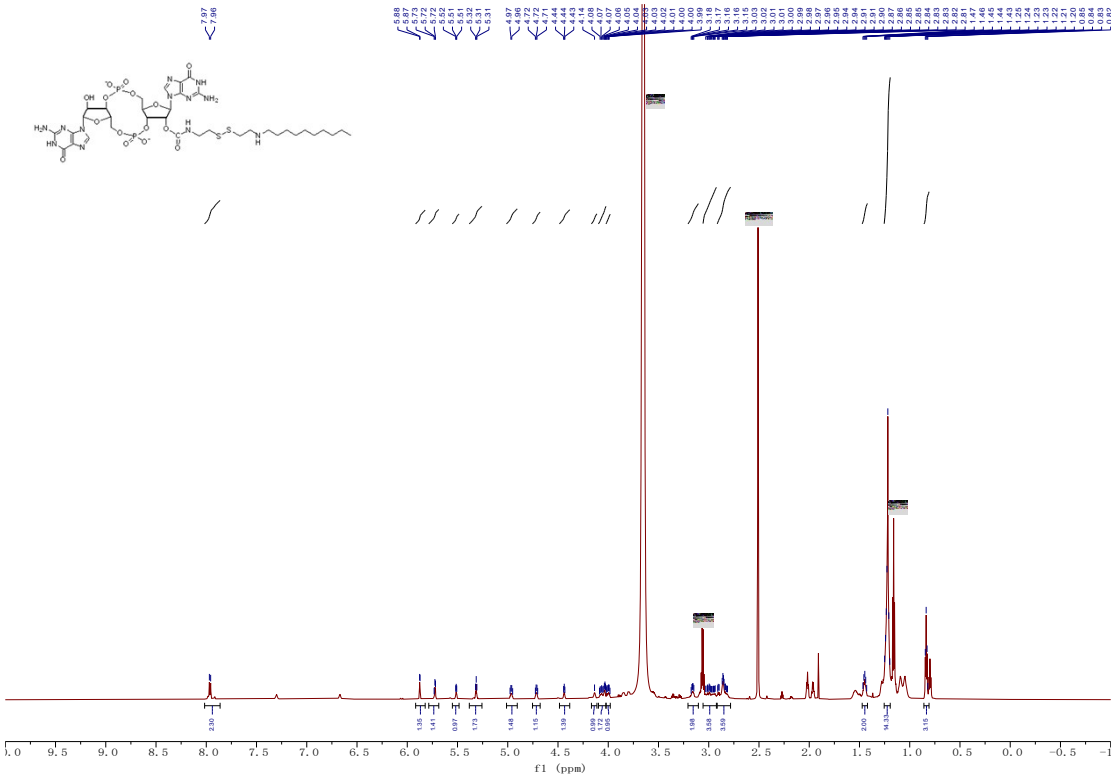

**Fig. S27.** $^{1}$H NMR (800 MHz, DMSO-$d_6$) spectra of **CDG-1C10**.

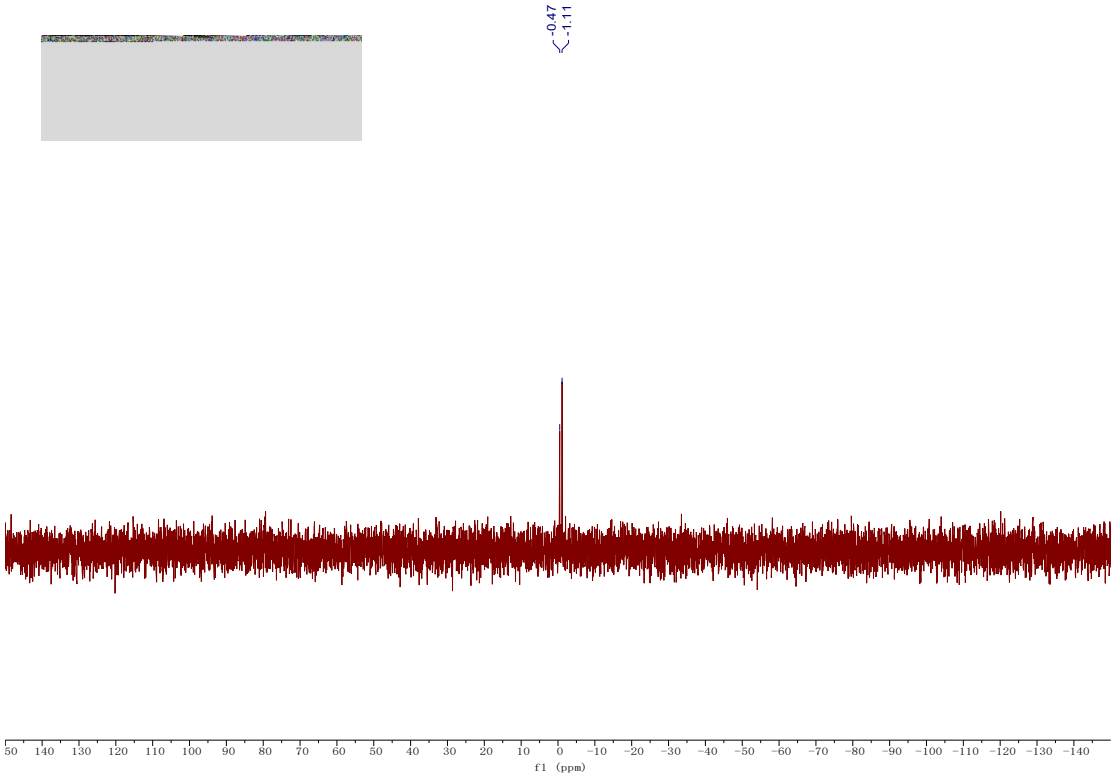


**Fig. S28.** $^{31}$P NMR (162 MHz, DMSO-$D_6$) spectra of **CDG-1C10**.

**CDG-1C12**

**$^{1}$H NMR (800 MHz, DMSO-$d_6$)** δ 7.96 (s, 2H), 5.87 (d, $J$ = 3.0 Hz, 1H), 5.72 (d, $J$ = 4.1 Hz, 1H), 5.51 (t, $J$ = 4.1 Hz, 1H), 5.31 (t, $J$ = 5.2 Hz, 2H), 4.98 - 4.94 (m, 1H), 4.72 - 4.68 (m, 1H), 4.43 (t, $J$ = 4.7 Hz, 1H), 4.14 - 4.09 (m, 1H), 4.09 - 4.03 (m, 2H), 4.02 - 3.99 (m, 1H), 3.20 - 3.13 (m, 2H), 3.05 - 2.91 (m, 4H), 2.93 - 2.79 (m, 4H), 1.47 - 1.41 (m, 2H), 1.28 - 1.16 (m, 18H), 0.85 - 0.81 (m, 3H). **$^{31}$P NMR (162 MHz, DMSO-$D_6$)** δ -0.69, -1.22.

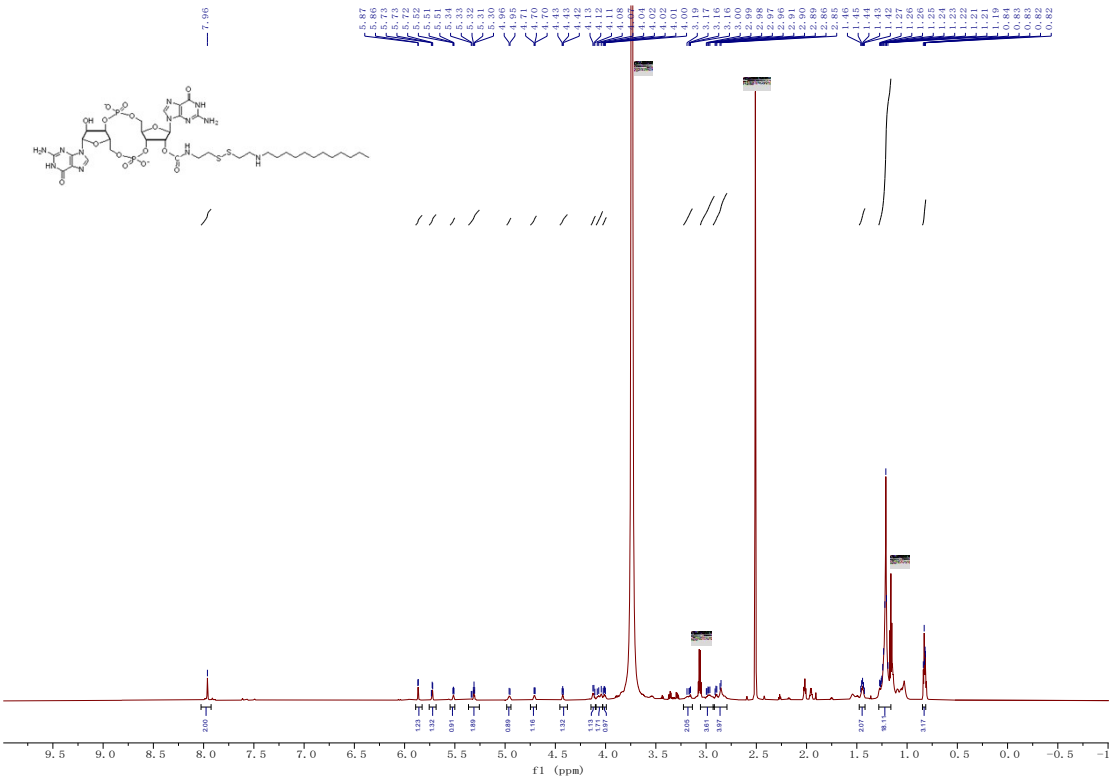

**Fig. S29.** $^{1}$H NMR (800 MHz, DMSO-$d_6$) spectra of **CDG-1C12**.

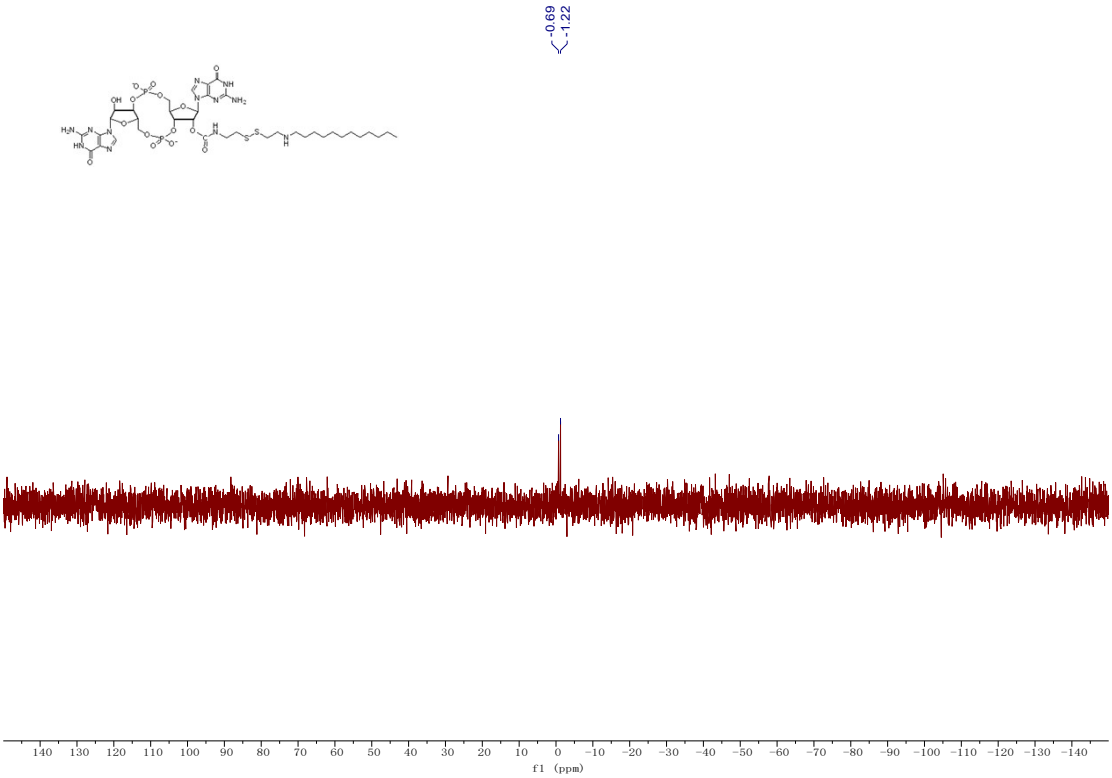

**Fig. S30.** $^{31}$P NMR (162 MHz, DMSO-$D_6$) spectra of **CDG-1C12**.

**CDG-1C14**

**$^{1}$H NMR (800 MHz, DMSO-$d_6$)** δ 7.97 (s, 1H), 7.94 (s, 1H), 5.88 (d, $J$ = 3.2 Hz, 1H), 5.72 (d, $J$ = 4.9 Hz, 1H), 5.54 – 5.49 (m, 1H), 5.31 (t, $J$ = 5.2 Hz, 2H), 5.00 – 4.93 (m, 1H), 4.73 – 4.69 (m, 1H), 4.44 (t,

$J$ = 5.0 Hz, 1H), 4.16 – 4.11 (m, 1H), 4.09 – 4.01 (m, 2H), 4.01 – 3.95 (m, 1H), 3.21 – 3.09 (m, 2H), 3.02 – 2.89 (m, 4H), 2.89 – 2.80 (m, 4H), 1.48 – 1.42 (m, 2H), 1.35 – 1.18 (m, 22H), 0.84 (td, $J$ = 7.1, 3.6 Hz, 3H). **$^{31}$P NMR (243 MHz, DMSO-$D_6$)** δ -0.89, -1.55.

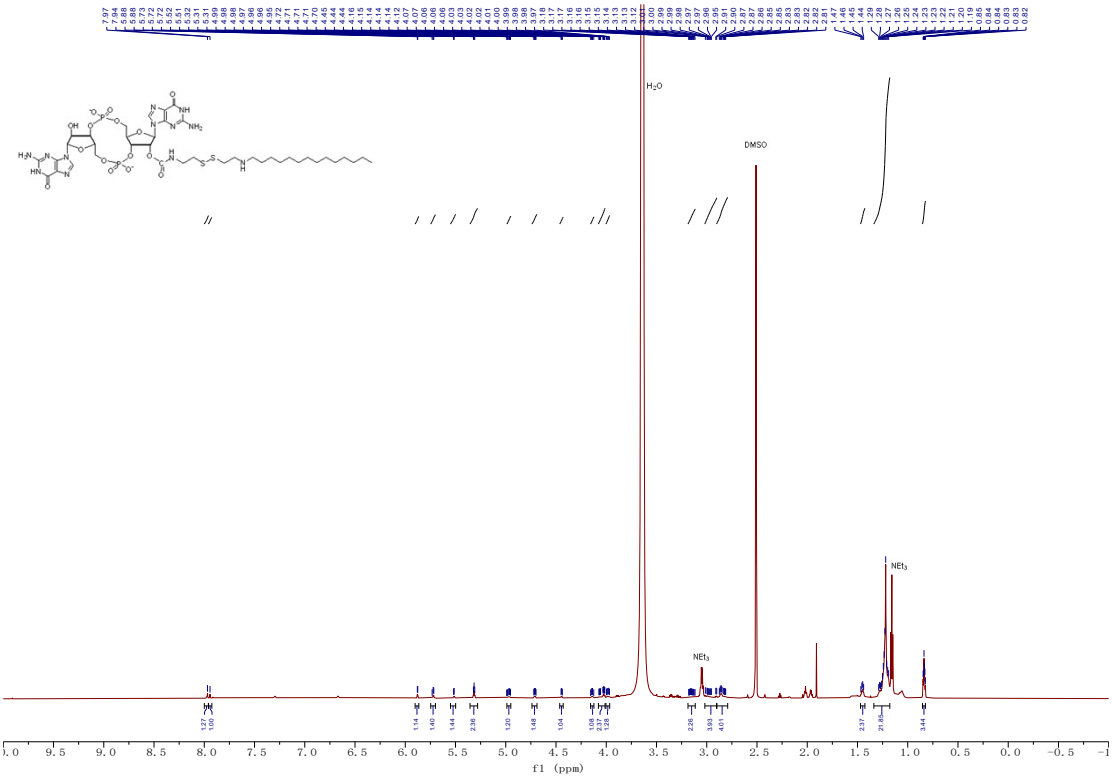


**Fig. S31.** $^{1}$H NMR (800 MHz, DMSO-$d_6$) spectra of **CDG-1C14**.

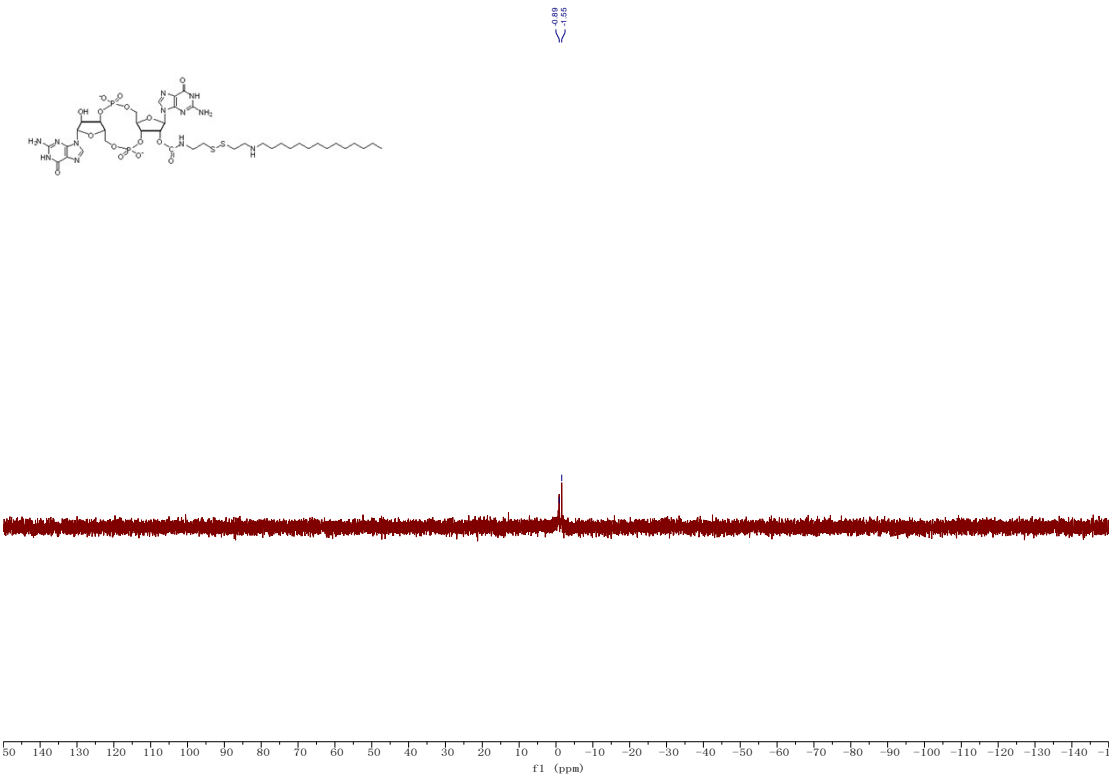


**Fig. S32.** $^{31}$P NMR (162 MHz, DMSO-$D_6$) spectra of **CDG-1C14**.

## 6. HPLC spectra of compounds

HPLC spectra for **CDG-1C8-CDG-1C14** (YMC analytic C8 column, 0.8 mL/min, gradient is 5 % to 80 % of solution B in solution A for 30 min).

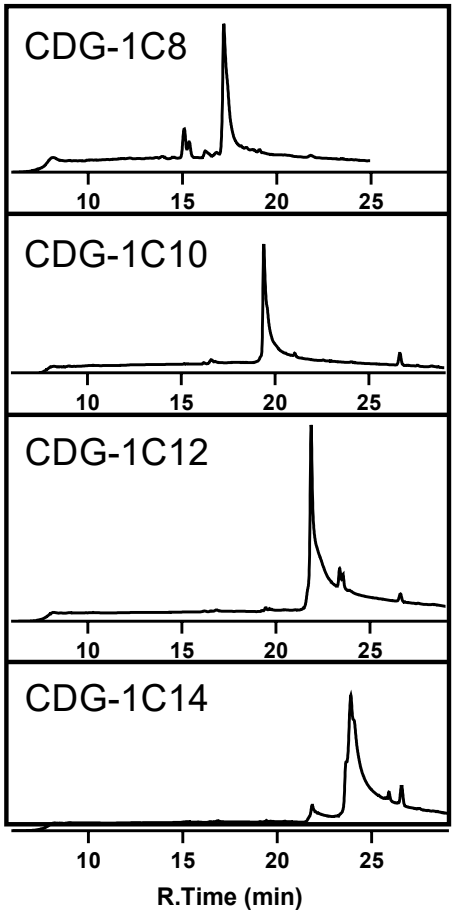


**Fig. S33.** HPLC spectra of **CDG-1C8-CDG-1C14**.

## 7. MS spectra of compounds

ESI-MS data for compound **1C8-1C14, CDG and CDG-1C8-CDG-1C14**

**1C8** $C_{12}H_{28}N_2S_2$ calculated: 264.17 [M], found: 265.28 $[M+H]^+$

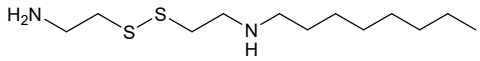


Chemical Formula: $C_{12}H_{28}N_2S_2$
Exact Mass: 264.17
Molecular Weight: 264.49

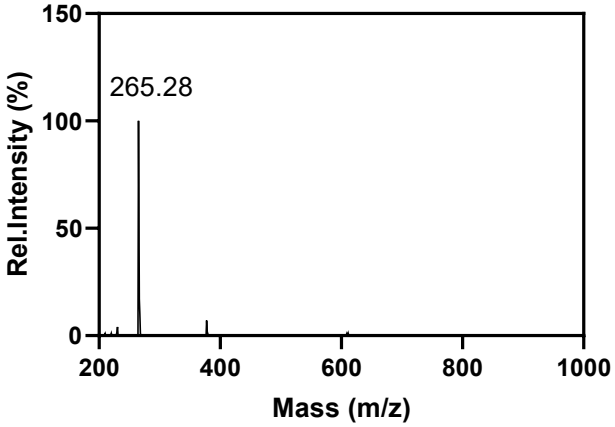


**Fig. S34.** ESI-MS spectra of **1C8.**

**1C10** $C_{14}H_{32}N_2S_2$ calculated: 292.20 [M], found: 293.30 $[M+H]^+$

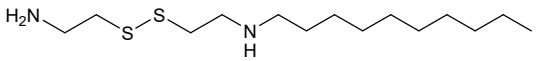


Chemical Formula: $C_{14}H_{32}N_2S_2$
Exact Mass: 292.20
Molecular Weight: 292.54

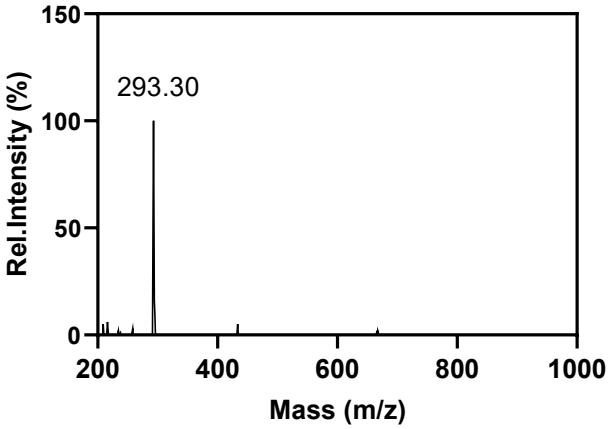


**Fig. S35.** ESI-MS spectra of **1C10.**

**1C12** $C_{16}H_{36}N_2S_2$ calculated: 320.23 [M], found: 321.27 $[M+H]^+$

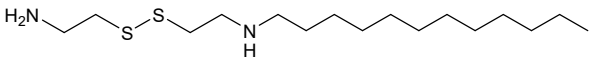

Chemical Formula: $C_{16}H_{36}N_2S_2$
Exact Mass: 320.23
Molecular Weight: 320.60

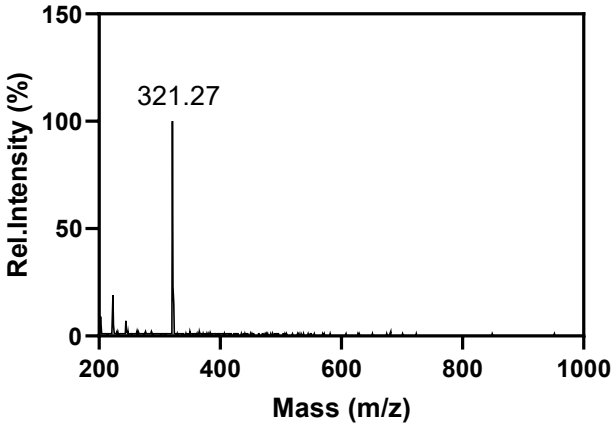


**Fig. S36.** ESI-MS spectra of 1C12.

**1C14** $C_{18}H_{40}N_2S_2$ calculated: 348.26 [M], found: 349.37 $[M+H]^+$

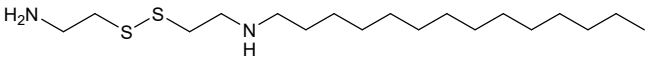

Chemical Formula: $C_{18}H_{40}N_2S_2$
Exact Mass: 348.26
Molecular Weight: 348.65

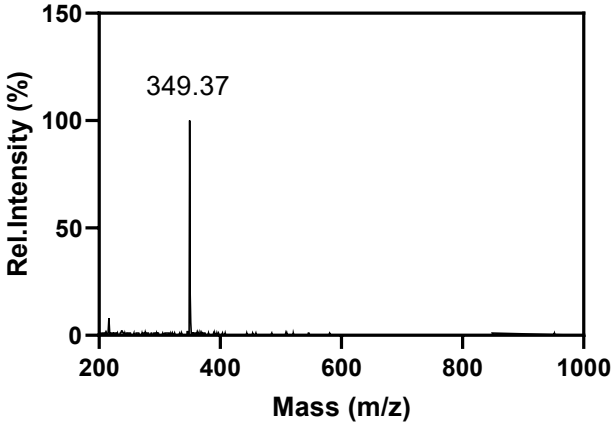


**Fig. S37.** ESI-MS spectra of **1C14.**

**CDG:** $C_{20}H_{24}N_{10}O_{14}P_2$ calculated: 690.09 [M], found: 689.10 $[M-H]^-$

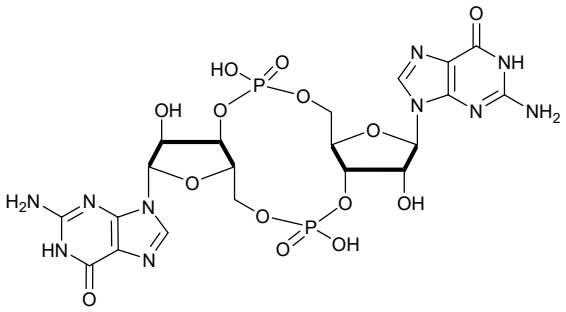

Chemical Formula: $C_{20}H_{24}N_{10}O_{14}P_2$
Exact Mass: 690.09
Molecular Weight: 690.42

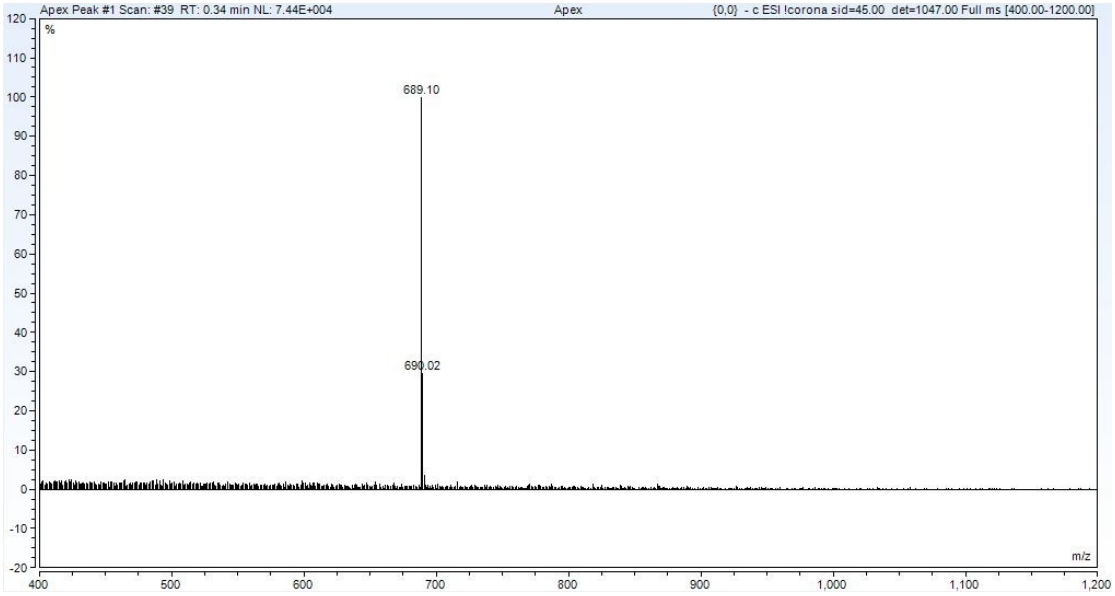


**Fig. S38.** ESI-MS spectra of **CDG.**

**CDG-1C8** $C_{33}H_{50}N_{12}O_{15}P_2S_2$ calculated: 980.24 [M], found: 981.35 $[M+H]^+$, 1082.52 $[M+(CH_3CH_2)_3N+H]^+$

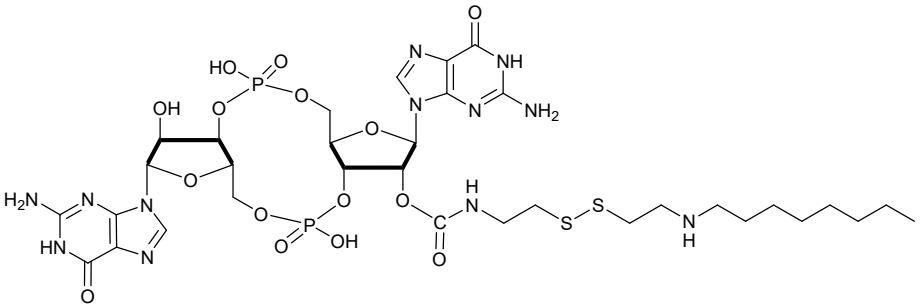

Chemical Formula: $C_{33}H_{50}N_{12}O_{15}P_2S_2$
Exact Mass: 980.24
Molecular Weight: 980.90

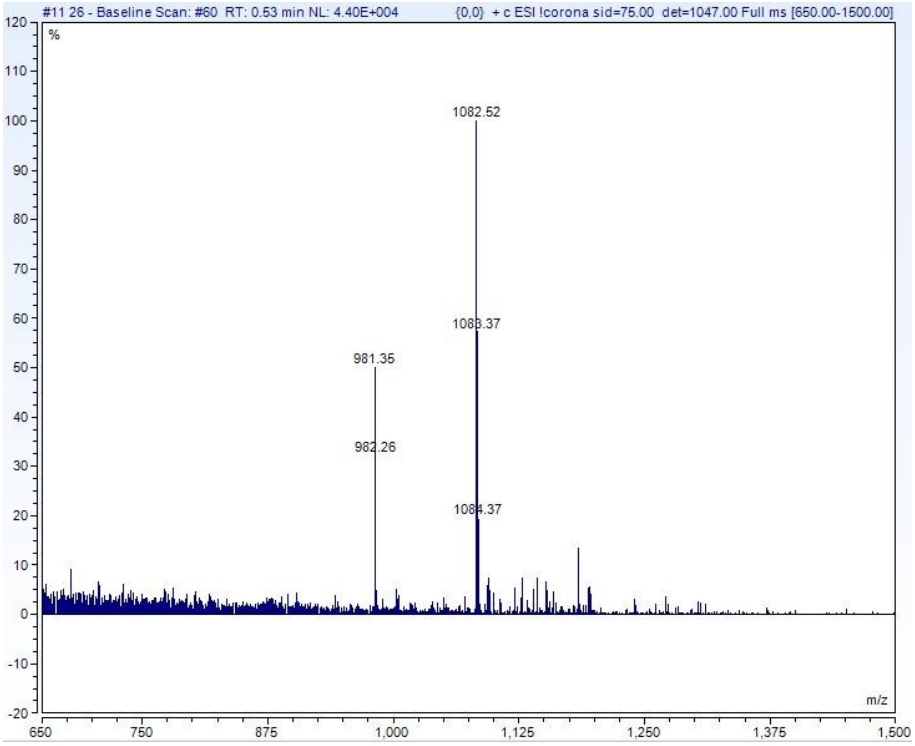


**Fig. S39.** ESI-MS spectra of **CDG-1C8.**

**CDG-1C10** $C_{35}H_{54}N_{12}O_{15}P_2S_2$ calculated: 1008.27 [M], found: 1007.44 $[M-H]^-$ 503.05 $[M-2H]^{2-}$

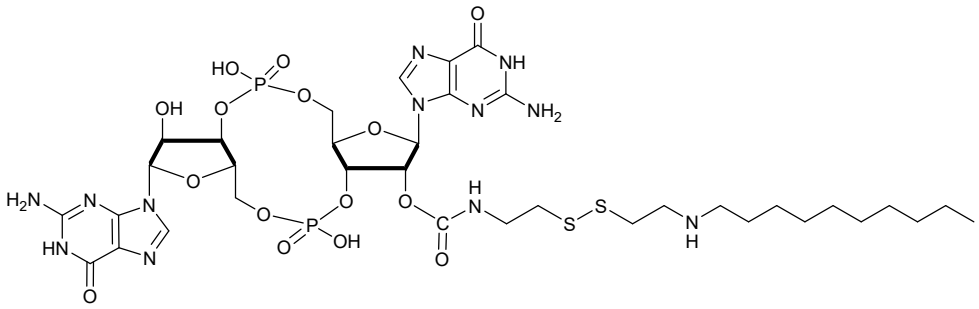

Chemical Formula: $C_{35}H_{54}N_{12}O_{15}P_2S_2$
Exact Mass: 1008.27
Molecular Weight: 1008.95

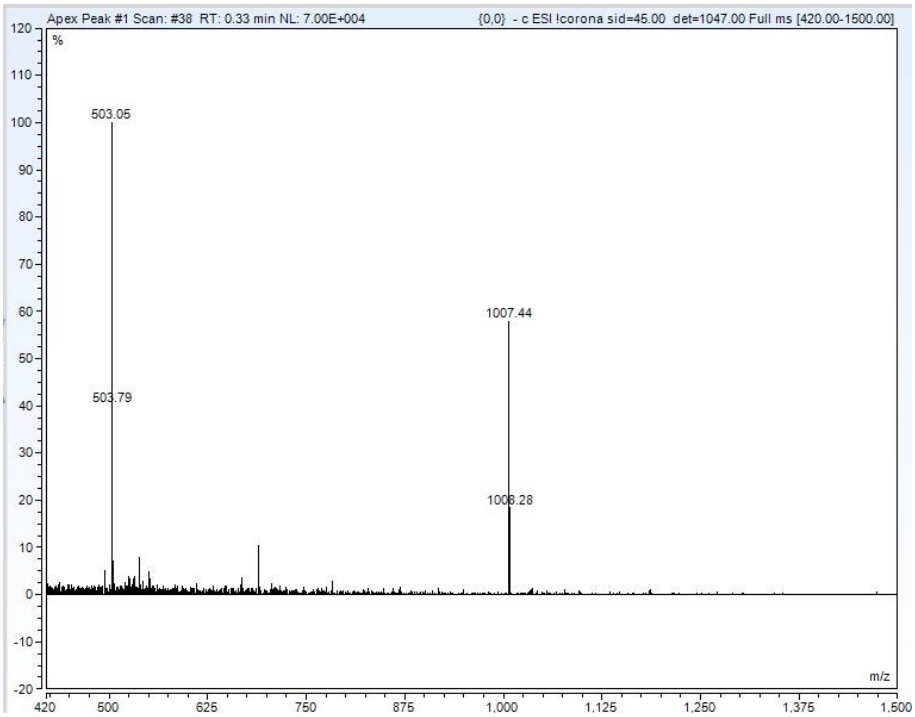


**Fig. S40.** ESI-MS spectra of **CDG-1C10.**

**CDG-1C12** $C_{37}H_{58}N_{12}O_{15}P_2S_2$ calculated: 1036.31 [M], found: 1037.00 $[M+H]^+$, 1138.59 $[M+(CH_3CH_2)_3N+H]^+$ 1239.63 $[M+2(CH_3CH_2)_3N+H]^+$

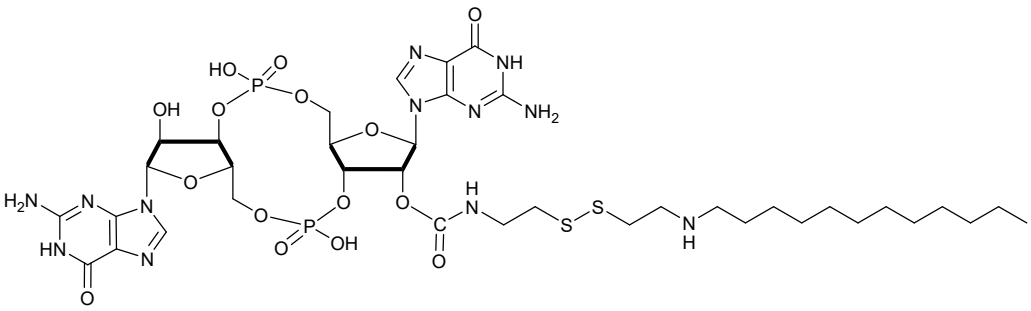

Chemical Formula: $C_{37}H_{58}N_{12}O_{15}P_2S_2$
Exact Mass: 1036.31
Molecular Weight: 1037.01

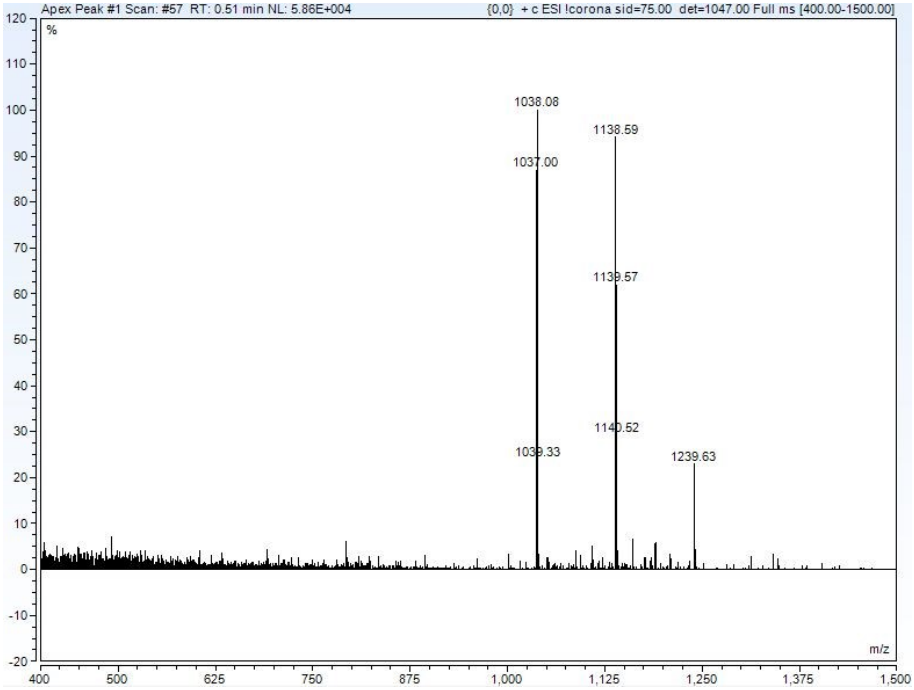


**Fig. S41.** ESI-MS spectra of **CDG-1C12.**

**CDG-1C14** $C_{39}H_{62}N_{12}O_{15}P_2S_2$ calculated: 1064.34 [M], found: 1063.28 $[M-H]^-$ 531.05 $[M-2H]^{2-}$

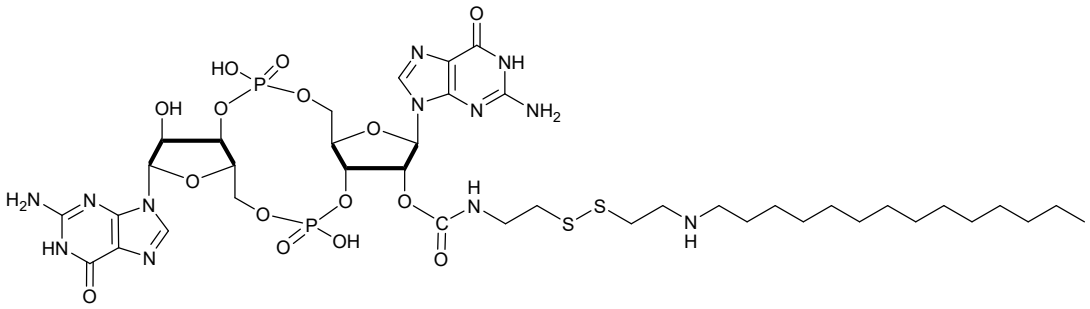

Chemical Formula: $C_{39}H_{62}N_{12}O_{15}P_2S_2$
Exact Mass: 1064.34
Molecular Weight: 1065.06

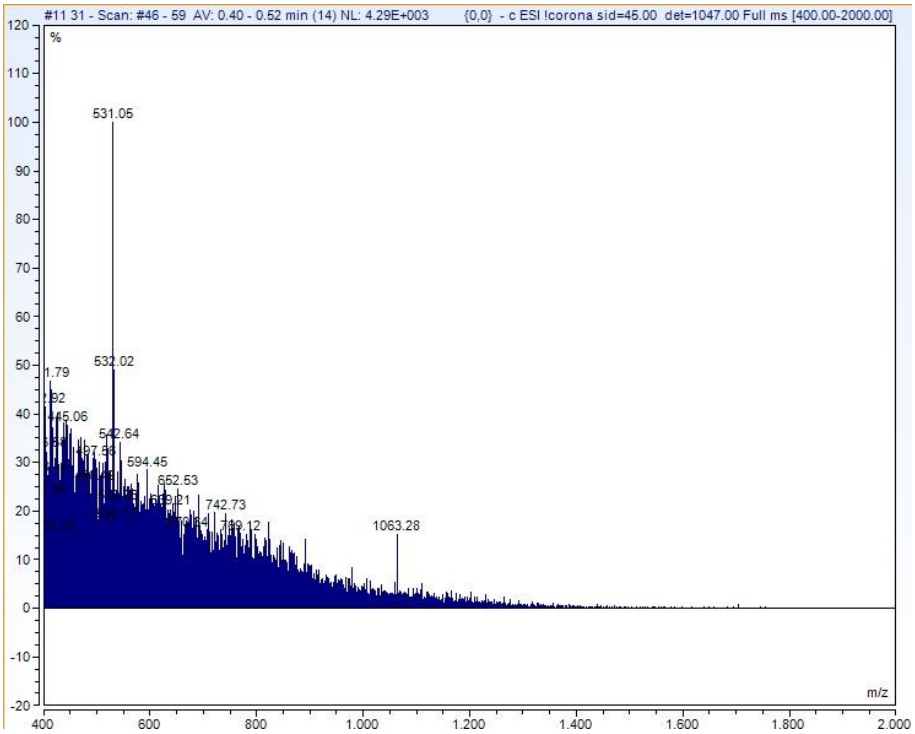


**Fig. S42.** ESI-MS spectra of **CDG-1C14**.

## 8. References

1. B. L. Gaffney, et al., *Org. Lett.*, 2010, **12**, 3269-3271.